



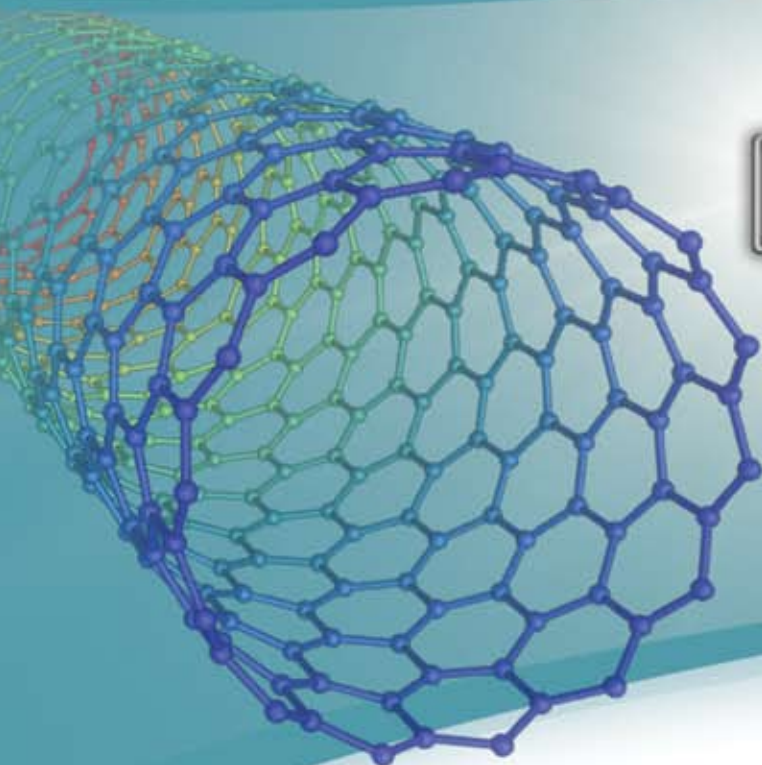
# Material Matters™

Chemistry Driving Performance

2007  
VOLUME 2  
NUMBER 1



## Advanced Applications of Engineered Nanomaterials



>scanning...



Inorganic Nanoparticles –  
Unique Properties  
Targeted to Applications

Quantum Dots –  
Emerging Optical  
Nanomaterials

Quantum Dots  
in Display Technology

Carbon Nanotube  
Electronics

Multifunctional  
Polymer-Clay  
Nanocomposites

Dendrimers for  
Drug Delivery

*Sensors, Electronics, Medicine ...  
breakthrough technologies born  
at the nanoscale*



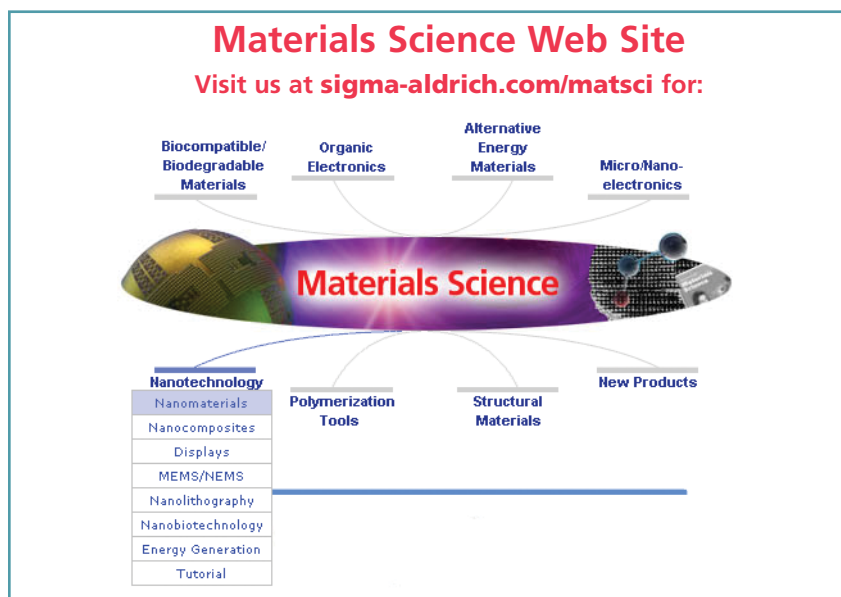
## Introduction

Welcome to the first installment of *Material Matters*™ for 2007. This thematic issue focuses on the emerging applications of nanomaterials. Nanomaterials are defined as substances with at least one dimension smaller than 100 nm. This definition encompasses many families of materials and collectively underscores the principle that properties of matter change at very small length scales. In this publication, scientists from the University of California-Davis discuss the relation between small sizes, unique properties, and applications of inorganic nanocrystals. Professor Philippe Guyot-Sionnest from the University of Chicago writes about the history, fascinating properties, and diverse applications of Quantum Dots, while Dr. Seth Coe-Sullivan, the CTO of QD-Vision, Inc., illustrates one successful application of Quantum Dots to make a new class of low-cost displays. Professor Moonsub Shim from the University of Illinois at Urbana-Champaign writes about the technical advancements and challenges of using single-wall carbon nanotubes to make nanoscale electronic circuits. Dr. Alexander Morgan from the University of Dayton gives a review of nanoclays, the class of nanomaterials most advanced in terms of commercially realized applications. Finally, researchers from Dendritic Nanotechnologies, Inc. illustrate the use of kits of structurally related dendrimers as tools for solubilization and controlled release of drugs.

Research excitement brought about by the realization that small size translates to unique properties of matter is now borne out in many diverse nanomaterials, some of which continue to stimulate new discoveries while others are already near the stage of commercialization in products promising to improve everyday life.

Our mission at Sigma-Aldrich is to inspire and advance your research, helping you to make the discoveries that will make life better. We hope that the articles and Sigma-Aldrich products featured in this issue will help you in your work. Please contact the Sigma-Aldrich Materials Science Team at [matsci@sial.com](mailto:matsci@sial.com) if you need a nanomaterial that you cannot find in our catalog. We will be delighted to give it careful consideration.

Ilya Koltover, Ph.D.  
Materials Science  
Sigma-Aldrich Corporation



### About Our Cover

Carbon nanotubes (CNTs) came to embody much of what is unique about nanomaterials. In his article on page 16, Professor Shim describes how the properties of seemingly similar CNTs can be dramatically altered by slight changes in their structure and environment. Could this variability be controlled or harnessed in applications? The cover depicts one such application where the environmental responsiveness of CNTs is used to create ultra-sensitive detectors that can "fingerprint" biomolecules and environmental contaminants. Imagine a tiny sensor that can ID an individual, detect disease, or regulate delivery of a vital drug. This is just one example where research succeeds in opening up new technologies enabled by materials with structure engineered at the nanoscale.

**Aldrich Chemical Co., Inc.**  
**Sigma-Aldrich Corporation**  
6000 N. Teutonia Ave.  
Milwaukee, WI 53209, USA

#### To Place Orders

Telephone 800-325-3010 (USA)  
FAX 800-325-5052 (USA)

#### Customer & Technical Services

Customer Inquiries 800-325-3010  
Technical Service 800-231-8327  
SAFC™ 800-244-1173  
Custom Synthesis 800-244-1173  
Flavors & Fragrances 800-227-4563  
International 414-438-3850  
24-Hour Emergency 414-438-3850  
Web Site [sigma-aldrich.com](http://sigma-aldrich.com)  
Email [aldrich@sial.com](mailto:aldrich@sial.com)

#### Subscriptions

To request your **FREE** subscription to *Material Matters*, please contact us by:

Phone: 800-325-3010 (USA)  
Mail: **Attn: Marketing Communications**  
**Aldrich Chemical Co., Inc.**  
**Sigma-Aldrich Corporation**  
**P.O. Box 355**  
**Milwaukee, WI 53201-9358**  
Email: [sams-usa@sial.com](mailto:sams-usa@sial.com)

International customers, please contact your local Sigma-Aldrich office. For worldwide contact information, please see back cover.

*Material Matters* is also available in PDF format on the Internet at [sigma-aldrich.com/matsci](http://sigma-aldrich.com/matsci).

Aldrich brand products are sold through Sigma-Aldrich, Inc. Sigma-Aldrich, Inc. warrants that its products conform to the information contained in this and other Sigma-Aldrich publications. Purchaser must determine the suitability of the product for its particular use. See reverse side of invoice or packing slip for additional terms and conditions of sale.

All prices are subject to change without notice.

*Material Matters* is a publication of Aldrich Chemical Co., Inc. Aldrich is a member of the Sigma-Aldrich Group. © 2007 Sigma-Aldrich Co.

## Inorganic Nanoparticles — Unique Properties and Novel Applications



Professors Mark Asta,<sup>1</sup> Susan M. Kauzlarich,<sup>2</sup> Kai Liu,<sup>3</sup> Alexandra Navrotsky,<sup>4,1</sup> and Frank E. Osterloh<sup>2</sup>  
 Departments of Chemical Engineering and Materials Science,<sup>1</sup> Chemistry,<sup>2</sup> Physics,<sup>3</sup> and Thermochemistry Facility and NEAT ORU,<sup>4</sup> University of California, Davis

### Introduction

Inorganic particles often exhibit novel physical properties as their size approaches nanometer scale dimensions. For example, the unique electronic and optical properties of nanocrystalline quantum dots may lead to future applications in electro-optic devices and biomedical imaging.<sup>1</sup> For many advanced and diverse applications, ranging from chemical sensing to magnetic recording, current research is increasingly focused on exploiting the high surface-to-volume ratios of nanoparticles as a framework for the assembly of complex nanomaterials. Structures including core/shell nanoparticles and multicomponent hierarchical assemblies can exhibit enhanced properties and new functionality arising from the close proximity of chemically-distinct, nanostructured components. This article highlights the rich variety of structures and properties that can be realized in materials based on inorganic nanoparticles, and points to outstanding fundamental questions raised in controlling these properties. These issues are discussed in the framework of a few illustrative examples for insulating and metallic nanoparticles, taken from the collaborative interdisciplinary research of faculty at UC Davis, interacting through the Nanomaterials in the Environment Agriculture and Technology (NEAT) organized research unit (<http://neat.ucdavis.edu>).

To fully appreciate the origin of their unique structures and physical properties, it is important to note that nanoparticles are different from bulk materials not just because they are small but also because a large fraction of their volume is within “hailing distance” of the surface (**Figure 1**). Thus, they can carry “heavy loads” of surface coatings, regions that are structurally and compositionally different from the bulk. These can be rearranged (relaxed) parts of the nanoparticle structure itself, a shell of solid of different composition, or adsorbed layers of water, inorganic or organic molecules. The adsorbed layers can be used as “linkages” to build novel hierarchical structures. The fundamental complexities in structure, bonding, and interfacial interactions between a particle, its coating, and its neighboring environment, can be exploited to derive unique properties for many potential applications.

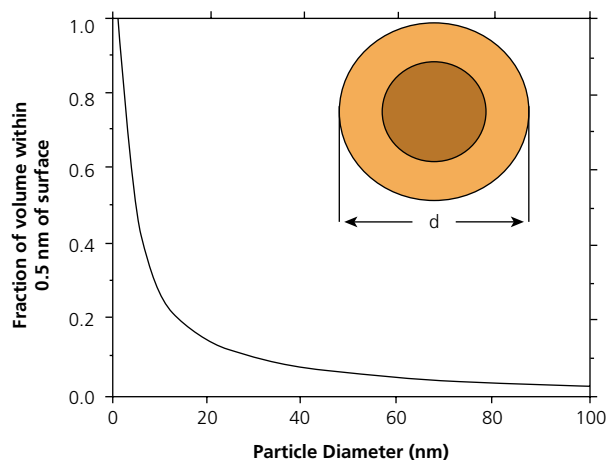


**Figure 1.** Fraction of volume of a particle of diameter  $d$  that lies within 0.5 nm of its surface. The lighter shell represents either that fraction or, alternately, the volume of a 0.5 nm coating on a particle of diameter  $d=1.5$  nm. Figure modified from Ref. 15.

### Complex Multi-phase Materials

Consider as a first example the variety of structures and applications associated with oxide nanoparticles. Taking iron oxides and oxyhydroxides as a specific example, the first thing to note is that these materials exist in a rich variety of polymorphs.<sup>2</sup> The common anhydrous iron oxide is hematite,  $\alpha\text{-Fe}_2\text{O}_3$ , a common iron ore and red paint pigment. Magnetite,  $\text{Fe}_3\text{O}_4$ , is a spinel and forms the basis of numerous magnetic materials and devices, while  $\gamma\text{-Fe}_2\text{O}_3$ , maghemite, has a defect spinel structure. Oxyhydroxides include goethite, lepidocrocite, akaganeite, ferrihydrite, and green rusts. The oxides and oxyhydroxides often consist of nanoparticles, both in nature and in synthetic materials. Iron oxide particles of various sizes are important as magnetic recording materials, ferrofluids, pigments, corrosion products, and in the transport of nutrients and contaminants (heavy metals and radionuclides) in the environment. The magnetic properties of magnetite and maghemite are also of great interest for biological applications. However, the corrosion sensitivity of magnetite and difficulties in permanently attaching biomolecules to the nanoparticle surface are significant obstacles for such uses. These problems can be overcome by coating the magnetic nanoparticle with a shell, which protects the core from oxidation and corrosion, and additionally, provides a platform for chemical functionalization, thus making the particles potentially bio-compatible. Such core/shell particles can be prepared, for example, by using two successive reverse micelle reactions.<sup>3</sup>

For questions, product data, or new product suggestions, please contact the Materials Science team at [matsci@sial.com](mailto:matsci@sial.com).

Core/shell structured magnetic nanoparticles are currently of interest for a wide variety of applications.<sup>4</sup> For example, magnetic-core/Au-shell structured nanoparticles, due to the possibility of remote magnetic manipulation, may be used in biological applications for magnetic resonance imaging (MRI), cell tagging and sorting, hyperthermia treatment, and targeted drug delivery.<sup>5-7</sup> To date, several different types of magnetic core/shell nanoparticles have been reported, including Fe/Au, Fe<sub>3</sub>O<sub>4</sub>/Au, and FeCo/(Au,Ag) nanoparticles.<sup>3,8-10</sup> An example of Au-coated Fe nanoparticles is shown in **Figure 2**.<sup>3,5,11,12</sup> Magnetic hard/soft core/shell nanoparticles are another type of technologically important nanostructure. Nanoparticles with high magnetocrystalline anisotropy, such as FePt or CoPt in the L1<sub>0</sub> phase, may be self-assembled into arrays and used as future generation patterned magnetic recording media with Terabit/in<sup>2</sup> density.<sup>13</sup> Core/shell structures coupling such magnetic hard phases with magnetic soft (e.g. Fe<sub>3</sub>Pt) phases may be used to achieve a large energy product for permanent magnet applications.

In these areas of research, the core/shell structure, particle size, shape and surface properties are important. For example, for magnetic recording applications using each high-anisotropy magnetic nanoparticle as a single bit, minimal dispersion in the size and shape distributions (<10%) are essential. Iron oxides such as Fe<sub>2</sub>O<sub>3</sub>, Fe<sub>3</sub>O<sub>4</sub>, and MFe<sub>2</sub>O<sub>4</sub> (M=Fe, Co, Mn) can be prepared as monodisperse surface derivatized nanoparticles.<sup>14</sup> Progress has also been made with the production of Co and Fe nanoparticles, as well as nanorods prepared by solution methods. In spite of these advancements and exciting attributes, core/shell structured nanoparticles present enormous synthetic challenges, particularly in terms of the growth mechanisms of the core/shell structures and independent control over core/shell dimensions. Detailed characterization of the core/shell structure, optimization of the core and shell to achieve the desired properties, and their applications in biology or technology are yet to be systematically demonstrated.

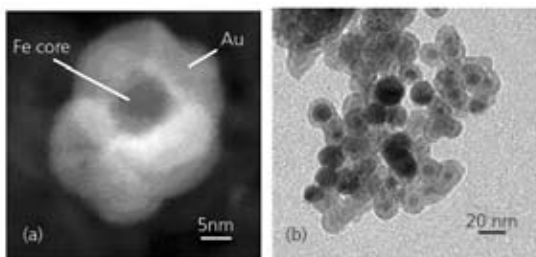


**Figure 2.** (a) Z-Contrast image of an Au-coated Fe nanoparticle obtained by scanning transmission electron microscopy. (b) Transmission electron microscopy image of Au-coated Fe nanoparticles.

### Fundamental Chemistry and Physics

The applications above all require understanding of the fundamental physics and chemistry of these complex nanostructures. For example, the competition between surface and bulk contributions to the energy of a particle can lead to the thermodynamic stabilization, at the nanoscale, of crystal structures (polymorphs) that are metastable in the bulk.<sup>15-18</sup> This effect can have important consequences for engineering the physical, chemical, electronic, and magnetic properties of these inorganic materials.

Experimental calorimetric studies have provided data on the surface energies and hydration energies of iron oxides and oxyhydroxides.<sup>16</sup> **Figure 3** shows the enthalpy of various polymorphs relative to an assemblage of coarse hematite plus liquid water at 25 °C. One sees that goethite becomes energetically stable relative to hematite plus water at surface areas greater than about 15 m<sup>2</sup>/g (and probably is stable in free energy even at smaller surface areas because of entropy effects). Akaganeite becomes energetically stable relative to hematite plus water at areas greater than 35 m<sup>2</sup>/g and lepidocrocite at greater than 100 m<sup>2</sup>/g. Akaganeite becomes stable relative to goethite at surface areas greater than 250 m<sup>2</sup>/g. It is striking that the slope of the line relating enthalpy and surface area (proportional to surface energy) is much higher for the anhydrous phase hematite than for any of the hydrous phases; this seems to be a general trend also seen in the alumina system.<sup>15-19</sup> Furthermore, the more metastable a polymorph is, the lower is its surface energy, a general trend seen not just in the iron oxides but in alumina, titania, and zirconia.<sup>15</sup> These complex crossovers in energetics can explain the synthesis and coarsening behavior of iron oxide nanoparticles, both in nature and in the laboratory. The capability of such particles to carry heavy metals such as lead or uranium, or organic pollutants, depends on the crystallographic nature of the particle as well as its surface area. Similarly the magnetic properties depend on phase as well as size.

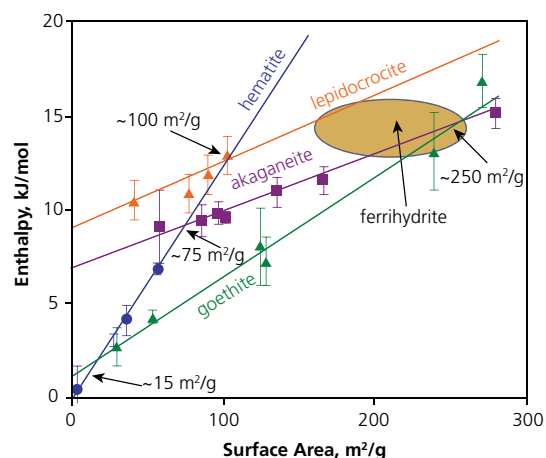


**Figure 3.** Calorimetrically measured enthalpies relative to coarse hematite plus liquid water  $\frac{1}{2}(\text{Fe}_2\text{O}_3 + \text{H}_2\text{O})$  for oxyhydroxides and fine grained hematite versus surface area (m<sup>2</sup>/g). The points are experimental data and the ellipse indicates the range for various ferrihydrite samples studied. Figure summarizes data taken from Refs. 16-18.

In addition to providing the framework for constructing “phase diagrams” to predict equilibrium nanoparticle structures as a function of their size, the measured energetics provide direct benchmarking of computational results for surface structure and energetics. Atomic-scale computer simulations are increasingly used to derive detailed insights into the energetic and kinetic factors governing structural transitions

and stability in inorganic nanoparticles. An example is illustrated in **Figure 4**, taken from recent Monte-Carlo simulations of FePt nanoparticles.<sup>20</sup> Due to their anomalously large magnetic anisotropy energies (MAE), and the associated very small critical sizes for superparamagnetism, FePt compounds are considered to be among the most promising candidate materials for future ultra-high-density magnetic recording devices.<sup>21</sup> To achieve the high MAE values associated with their bulk counterparts, it is critical to form FePt nanoparticles in their equilibrium tetragonal phase ( $L1_0$ ). As synthesized, FePt nanoparticles generally form in the metastable cubic ( $A1$ ) phase that is magnetically soft, and a post-synthesis annealing step is required to induce formation of the magnetically hard tetragonal phase. Experimental studies have demonstrated a pronounced size dependence of the cubic-tetragonal, order-disorder transition temperature ( $T_0$ ), which is significantly reduced in particles with nanometer-scale diameters.<sup>22</sup> Computer simulations suggest that the origin of this effect stems from a surface-induced disordering of the structure, whereby the particle becomes "wetter" by a disordered surface region at temperatures well below the bulk value of  $T_0$  (Figure 4). The propensity for this surface-induced disordering is significantly affected by the crystalline orientation of the surface facets and the degree of segregation of Fe or Pt onto the particle surface. These findings suggest that surface coatings, as well as control of particle morphology through the synthesis methods described above, are highly effective ways to manipulate the ordering tendencies and stability of the high-magnetic-anisotropy phase down to small particle sizes.

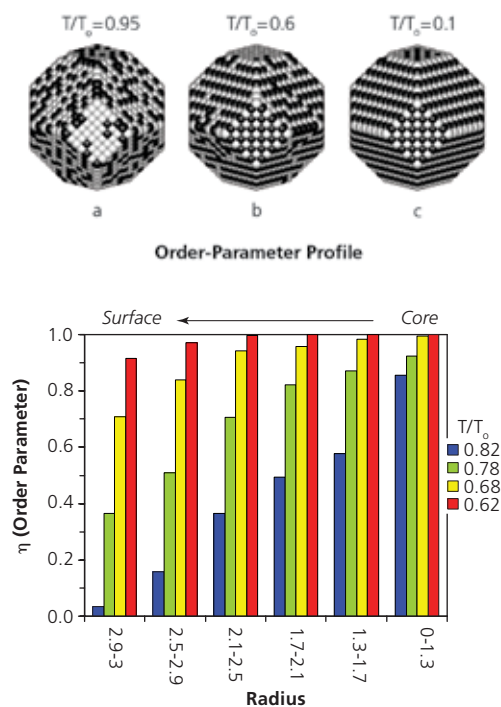


**Figure 4.** Monte-Carlo simulation snapshots (top) illustrate the nature of the equilibrium atomic ordering transition in Fe-Pt nanoparticles with a characteristic size of 4.79 nm. The lower figure plots order-parameter profiles, as a function of radial distance within the nanoparticle, at different temperatures, illustrating a disordering transition that is surface induced. The top panel is reprinted from Ref. 20, with permission from Elsevier.

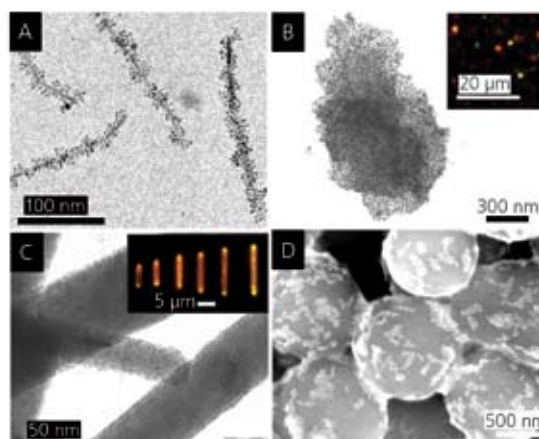


**Figure 5.** A.  $\text{LiMo}_3\text{Se}_3/\text{Fe}_3\text{O}_4$  nanocompasses. B.  $\text{Ca}_2\text{Nb}_3\text{O}_{10}/\text{Au}$  nanoparticle mirrors (inset: optical micrograph showing reflection). C.  $\text{ZnO}/\text{CdSe}$  light emitters (inset: optical micrograph showing directional fluorescence). D.  $\text{SiO}_2/\text{Au}$  thiol sensors (after reaction with dodecanethiol).

### Surface Coatings and Hierarchical Assemblies

Surface coatings also provide a pathway to chemically assemble more complex nanostructures, for example dual-component structures for advanced applications. Examples of discrete dual-component structures with potential uses as optical waveguides, magnetic actuators, and chemical sensors are shown in **Figure 5**.<sup>23</sup> In the first example (Figure 5A), magnetite nanoparticles are covalently linked to  $\text{LiMo}_3\text{Se}_3$  nanowire bundles to produce ~400 nm long needle-like structures. According to temperature-dependent magnetization measurements, these structures exhibit a magnetic anisotropy along the longer axis that is caused by magnetic dipole interactions between the magnetite nanoparticles. As a result, the structures have the ability to align with weak magnetic fields, and function as nanoscale compasses<sup>24</sup> or magnetic actuators. Figure 5B shows a nanostructure composed of gold nanoparticles covalently linked to a colloidal plate made of  $\text{HCa}_2\text{Nb}_3\text{O}_{10}$ . In this configuration, the nanoparticle structure serves as a microscale mirror with the ability to reflect light into discrete directions.<sup>25</sup> The red, green and yellow reflections that result from illuminating a sample of these dispersed mirrors with two lasers are shown in the inset. Another type of microscale waveguide is depicted in Figure 5C. Here hexagonal rod-shaped zinc oxide microcrystals serve as supports for covalently attached CdSe nanoparticles.<sup>26</sup> The formed microstructure produces a directional emission at the rod ends when illuminated with light in the ultraviolet. This emission arises from the fluorescence of the CdSe quantum dots, and it is waveguided by the ZnO microcrystal. The wavelength of the fluorescence is tunable with the size of the CdSe nanoparticles. Nanostructures in Figures 5B and C should be of interest for spatial light modulators, optical switches, and light-emitting devices. As a final example illustrating potential applications of hybrid multicomponent nanostructures, electrostatically bonded  $\text{SiO}_2$ -Au clusters (Figure 5D) can be used for qualitative and selective nanomolar detection or aliphatic thiols of varying hydrocarbon chain lengths (C2-C18).<sup>27</sup> Reaction with the thiols causes a change of the binding between  $\text{SiO}_2$  and Au particles, which lead to characteristic structural and color changes of the clusters. Because these sensors do not require additional components for signal transduction and processing, the submicrometer-sized clusters are true examples of nanoscale sensors.

The examples above illustrate that structure and properties of materials can change dramatically at the nanoscale, and that these changes can be driven by thermodynamic factors as well as controlled by the kinetics of nanoparticle nucleation and growth. The assembly of complex hierarchical nanostructures, leading to new materials and devices, depends on interactions at the molecular scale, particularly at the surfaces and interfaces of the nanoparticles. Fundamental understanding of these interactions requires

a combination of experimental and theoretical techniques, while characterization of the nanostructures formed requires structural analysis (electron microscopy and other methods) and modeling at larger length scales. Driven by the promise of diverse and exciting applications, this field of research offers challenges to develop these methodologies and integrate them into a holistic picture spanning length scales from tenths to thousands of nanometers.

#### References:

(1) Guyot-Sionnest, P., *Quantum Dots: An Emerging Class Of Soluble Optical Nanomaterials*, *Material Matters*, **2007**, Vol 2 No 1, 10. (2) Cornell, R.M. and Schwertmann, U., *The Iron Oxides: Structure, Properties, Occurrence, Uses*, **1996**, VCH, Germany. (3) Cho, S.-J., Kauzlarich, S.M., Olamit, J., Liu, K., Grandjean, F., Rebbouh, L., Long, G.J., *J. Appl. Phys.*, **2004**, 95, 6804. (4) Ross, C., *Annual Review of Materials Research*, **2001**, 31, 203. (5) Cho, S.J., Jarrett, B.R., Louie, A.Y., Kauzlarich, S.M., *Nanotechnology*, **2006**, 17, 640. (6) Niemeyer, C.M., *Angewandte Chemie, International Edition*, **2001**, 40, 4128. (7) Mornet, S., Vasseur, S., Grasset, F., Duguet, E., *Journal of Materials Chemistry*, **2004**, 14, 2161. (8) Carpenter, E.E., Sangregorio, C., O'Connor, C.J., *IEEE Transactions on Magnetics*, **1999**, 35, 3496. (9) Lyon, J.L., Fleming, D.A., Stone, M.B., Schiffer, P., Williams, M.E., *Nano Lett.*, **2004**, 4, 719. (10) Bai, J.M., Wang, J.P., *Appl. Phys. Lett.*, **2005**, 87, 152502. (11) Cho, S.J., Idrobo, J.C., Olamit, J., Liu, K., Browning, N.D., Kauzlarich, S.M., *Chem. Mater.*, **2005**, 17, 3181. (12) Liu, K., Cho, S., Kauzlarich, S.M., Idrobo, J.C., Davies, J.E., Olamit, J., Browning, N.D., Shahin, A.M., Long, G.J., Grandjean, F., *Mater. Res. Soc. Symp. Proc.*, **2006**, 887, 0887. (13) Sun, S.H., Murray, C.B., Weller, D., Folks, L., Moser,

A., *Science*, **2000**, 287, 1989. (14) Sun, S.H., Zeng, H., Robinson, D.B., Raoux, S., Rice, P.M., Wang, S.X., Li, G.X., *J. Am. Chem. Soc.*, **2004**, 126, 273. (15) Navrotsky, A., *Geochemical Transactions*, **2003**, 4, 34. (16) Majzlan, J., Schwertmann, U., Navrotsky, A., *Geochemical et Cosmochimica Acta*, **2004**, 69, 1039. (17) Mazeina, L., Navrotsky, A., *Clays and Clay Minerals*, **2005**, 53, 113. (18) Mazeina, L., Deore, S.W., Navrotsky, A., *Chemistry of Materials*, **2006**, 18, 1830. (19) Majzlan, J., Navrotsky, A., Casey, W.H., *Clays and Clay Minerals*, **2000**, 48, 699-707. (20) Yang, B., Asta, M., Mryasov, O.N., Klemmer, T.J., Chantrell, R.W., *Acta Mater.*, **2006**, 54, 4201. (21) Weller, D., Moser, A., Folks, L., Best, M.E., Lee, W., Toney, M.F., Schwickert, M., Thiele, J.U., Doerner, M.F., *IEEE Trans. Magn.*, **2000**, 36, 10. (22) Miyazaki, T., Kitakami, O., Okamoto, S., Shimada, Y., Akase, Z., Murakami, Y., Shindo, D., Takahashi, Y.K., Hono, K., *Phys. Rev. B*, **2005**, 72, 144419. (23) Osterloh, F.E., *Com. Inorg. Chem.*, **2006**, 27, 41. (24) Osterloh, F.E., Hiramatsu, H., Dumas, R.K., Liu, K., *Langmuir*, **2005**, 21, 9709. (25) Kim, J.Y., Osterloh, F.E., *J. Am. Chem. Soc.*, **2006**, 128, 3868. (26) Kim, J.Y., Osterloh, F.E., *J. Am. Chem. Soc.*, **2005**, 127, 10152. (27) Osterloh, F., Hiramatsu, H., Porter, R., Guo, T., *Langmuir*, **2004**, 20, 5553.

## Sonics and Materials Ultrasonic Processors

### Precise nanoparticle dispersal

POWERFUL

PRECISE

PRODUCTIVE

PREDICTABLE

The compact Sonics and Materials 20kHz ultrasonic processing unit can process samples from 250mL to several liters if using a continuous flow cell. These units are manufactured by the world leaders in ultrasonic technology and proven in real laboratory situations. When used with the stainless steel continuous flow cell they can process one or two low viscosity samples simultaneously up to 20 L/hour.

See our complete range of ultrasonic processors at [sigma-aldrich.com/Labware](http://sigma-aldrich.com/Labware)

Description	Prod. No.
500W processor, 220V	Z511471
500W processor, 110V	Z528897
750W processor, 220V	Z511463
750W processor, 110V	Z509302
Continuous flow cell, glass, up to 15 L/hour	Z645680
Low volume continuous flow cell, SS, up to 20 L/hour	Z562556



- Variable power output control
- Automatic tuning & frequency control
- Integrated temperature controller
- Consistent reproducibility
- Stores up to 10 procedures
- Real time display
- Control process time from 1 second to 10 hour

TO ORDER: Contact your local Sigma-Aldrich office (see back cover), call 1-800-325-3010 (USA), or visit [sigma-aldrich.com/matsci](http://sigma-aldrich.com/matsci).

## Nanoparticle Powders and Dispersions Available from Sigma-Aldrich

Sigma-Aldrich offers a broad range of research-grade nanoparticles spanning most of the Periodic Table. Available as nanopowders as well as dispersions and suspensions of functionalized particles, they are listed here in groups by the majority element in the particle composition.

Atomic No.	Element	Name	Particle Size (nm)	Nanopowder/Dispersion	Prod. No.
6	<b>C</b>	Carbon 99+%	30	nanopowder	<b>633100</b>
		Diamond 95+%	~3.2	nanopowder	<b>636444</b>
		Diamond 97+%	3.5-6.5	nanopowder	<b>636428</b>
12	<b>Mg</b>	Magnesium hydroxide 99.9%	<40	nanopowder	<b>632309</b>
		Magnesium hydroxide 99.9%	<40	nanopowder	<b>632309</b>
		Magnesium oxide	10-20	nanopowder	<b>549649</b>
		Magnesium aluminum spinel	<50	nanopowder	<b>677396</b>
13	<b>Al</b>	Aluminum, activated 99.5%	100	nanopowder	<b>653608</b>
		Aluminum nitride	<100	nanopowder	<b>593044</b>
		Aluminum oxide	40-50	nanopowder	<b>544833</b>
		Aluminum oxide whiskers (d x L)	2-4 X 2800	nanopowder	<b>551643</b>
		Aluminum oxide	<20	10% dispersion in water	<b>642991</b>
		Aluminum oxide	<20	5% dispersion in water	<b>643092</b>
		Aluminum titanate 98.5%	<20	nanopowder	<b>634131</b>
14	<b>Si</b>	Silicon 98+%	<100	nanopowder	<b>633097</b>
		Silicon carbide	45-55	nanopowder	<b>594911</b>
		Silicon nitride 98.5+%	15-30	nanopowder	<b>636703</b>
		Silicon nitride 98+%	<50	nanopowder	<b>634581</b>
		Silica (Silicon dioxide) 99.5%	10	nanopowder	<b>637246</b>
		Silica (Silicon dioxide) 99.5%	15	nanopowder	<b>637238</b>
		Silicon dioxide, alumina doped, >99.99%	<20	5% dispersion in water	<b>643130</b>
		Silicon dioxide, alumina doped	<20	10% dispersion in water	<b>643084</b>
		3-aminopropyl-(3-oxobutanoic acid)siloxy functionalized silica	15	2.5% dispersion in DMF	<b>660450</b>
		3-aminopropylsiloxy functionalized silica	15	3% dispersion in EtOH	<b>660442</b>
20	<b>Ca</b>	Calcium oxide	<160	nanopowder	<b>634182</b>
		Calcium titanate 99.9%	60-100	nanopowder	<b>633801</b>
		Calcium zirconate 99.7%	10-20	nanopowder	<b>631965</b>
		Calcium hydroxyapatite (HAp) > 97%	~160	nanopowder	<b>677418</b>
22	<b>Ti</b>	Titanium, activated 98.5%	100	dispersion in mineral oil	<b>513415</b>
		Titanium carbide 98+%	130	nanopowder	<b>636967</b>
		Titanium carbonitride (7:3) 97+%	50-80	nanopowder	<b>636940</b>
		Titanium carbonitride 97+%	50-80	nanopowder	<b>636959</b>
		Titanium(IV) oxide	<40	10% dispersion in water	<b>643017</b>
		Titanium(IV) oxide	<40	5% dispersion in water	<b>643114</b>
		Titanium(IV) oxide 99.7%	5-10	nanopowder	<b>637254</b>
		Titanium(IV) oxide 99.9%	60-100	nanopowder	<b>634662</b>
		Titanium oxide, 1% Mn doped	<100	nanopowder	<b>677469</b>
		Titanium silicon oxide 99.8%	5-20	nanopowder	<b>641731</b>
24	<b>Cr</b>	Chromium(III) oxide 99%	<40	nanopowder	<b>634239</b>
25	<b>Mn</b>	Manganese(II) titanium oxide	40-60	nanopowder	<b>634247</b>

For package size and prices, please visit [sigma-aldrich.com](http://sigma-aldrich.com).

For questions, product data, or new product suggestions,  
please contact the Materials Science team at [matsci@sial.com](mailto:matsci@sial.com).

Atomic No.	Element	Name	Particle Size (nm)	Nanopowder/Dispersion	Prod. No.
26	<b>Fe</b>	Iron, activated powder 99.5%	<100	dispersion in mineral oil	<b>513423</b>
		Iron(II,III) oxide 98+%	20-30	nanopowder	<b>637106</b>
		Iron(III) oxide	20-25	nanopowder	<b>544884</b>
		Magnetic Iron oxide	20-30	0.8 - 1.4% dispersion in heptane	<b>07318</b>
		Iron-nickel (55:45) alloy >97%	<100	nanopowder	<b>677426</b>
		Iron nickel oxide 98+%	20-30	nanopowder	<b>637149</b>
27	<b>Co</b>	Cobalt(II,III) oxide 99.8%	12-30	nanopowder	<b>637025</b>
		Cobalt aluminum oxide 99.9+%	<40	nanopowder	<b>633631</b>
28	<b>Ni</b>	Nickel, activated 99.9+%	<100	nanopowder	<b>577995</b>
		Nickel chromium oxide 99.6%	<40	nanopowder	<b>633976</b>
		Nickel cobalt oxide 99%	30-100	nanopowder	<b>634360</b>
		Nickel zinc iron oxide 99+%	40-60	nanopowder	<b>641669</b>
29	<b>Cu</b>	Copper 99.8%	<100	nanopowder	<b>634220</b>
		Copper(I) oxide	~225	1.5% dispersion in ethanol	<b>678945</b>
		Copper(II) oxide	30-40	nanopowder	<b>544868</b>
		Copper aluminum oxide 98.5%	40-60	nanopowder	<b>634301</b>
		Copper iron oxide 98.5%	60-100	nanopowder	<b>641723</b>
		Copper zinc iron oxide 98.5%	60-100	nanopowder	<b>641650</b>
		Copper-zinc (60:40) alloy	<100	nanopowder	<b>593583</b>
30	<b>Zn</b>	Zinc, activated 99+%	<100	nanopowder	<b>578002</b>
		Zinc oxide	50-70	nanopowder	<b>544906</b>
		Zinc oxide, doped with 6% Al, >97%	<50	nanopowder	<b>677450</b>
		Zinc titanate 99.5%	<40	nanopowder	<b>634409</b>
38	<b>Sr</b>	Strontium titanate 99.5+%	<100	nanopowder	<b>517011</b>
		Strontium ferrite 99.8%	60-100	nanopowder	<b>633836</b>
39	<b>Y</b>	Yttrium(III) oxide	25-30	nanopowder	<b>544892</b>
		Yttrium(III) oxide 99.9+%	<80	5% dispersion in water	<b>641901</b>
40	<b>Zr</b>	Zirconium(IV) oxide	25-30	nanopowder	<b>544760</b>
		Zirconium(IV) oxide	<150	10% dispersion in water	<b>643025</b>
		Zirconium silicate	25-30	nanopowder	<b>544760</b>
41	<b>Nb</b>	Niobium 99+ %	100	nanopowder	<b>593257</b>
42	<b>Mo</b>	Molybdenum, activated 99.8%	~100	nanopowder	<b>577987</b>
47	<b>Ag</b>	Silver 99.5%	70	nanopowder	<b>576832</b>
		Silver, activated 99%	~100	nanopowder	<b>484059</b>
		Silver	40	10% dispersion in ethylene glycol	<b>658804</b>
		Silver-copper (97.5:2.5) alloy	70	nanopowder	<b>576824</b>
		Silver-tin (97:3) alloy >97%	<100	nanopowder	<b>677434</b>
		Silver-platinum (95:5) alloy	100	nanopowder	<b>578533</b>
		Decanethiol derivatized silver nanoparticles	1-10 (90%)	0.1% dispersion in hexane	<b>673633</b>
		Dodecanethiol functionalized silver nanoparticles	10	0.25% dispersion in hexane	<b>667838</b>
49	<b>In</b>	Indium(III) hydroxide 99.99%	25-35	nanopowder	<b>637157</b>
		Indium(III) oxide 99.9%	<40	nanopowder	<b>632317</b>
		Indium-tin oxide	25-45	nanopowder	<b>544876</b>
		Indium-tin oxide	20-40	0.25% dispersion in isopropanol	<b>657212</b>
50	<b>Sn</b>	Tin, activated 99.7%	100	nanopowder	<b>576883</b>
		Tin(IV) oxide	5-20	nanopowder	<b>549657</b>

For package size and prices, please visit [sigma-aldrich.com](http://sigma-aldrich.com).

Atomic No.	Element	Name	Particle Size (nm)	Nanopowder/Dispersion	Prod. No.
51	<b>Sb</b>	Antimony(III) oxide	90-210	nanopowder	<b>637173</b>
		Antimony tin oxide 99.5+%	15-20	nanopowder	<b>549541</b>
56	<b>Ba</b>	Barium titanate(IV) 99+%	30-50	nanopowder	<b>467634</b>
		Barium ferrite 99.5%	40-60	nanopowder	<b>637602</b>
		Barium strontium titanium oxide 99.7%	<125	nanopowder	<b>633828</b>
		Barium zirconate 98.5%	<40	nanopowder	<b>631884</b>
57	<b>La</b>	Lanthanum oxide 99%	25-65	nanopowder	<b>634271</b>
58	<b>Ce</b>	Cerium(IV) oxide 99.95%	< 20	10% dispersion in water	<b>643009</b>
		Cerium(IV) oxide 99.95%	< 20	5% dispersion in water	<b>639648</b>
		Cerium aluminum oxide 99%	10-25	nanopowder	<b>637866</b>
		Cerium(IV)-zirconium(IV) oxide 99.0%	<20	nanopowder	<b>634174</b>
59	<b>Pr</b>	Praseodymium oxide 99%	<125	nanopowder	<b>634263</b>
62	<b>Sm</b>	Samarium oxide 99.9+%	40-80	nanopowder	<b>637319</b>
		Samarium(III) oxide	<80	5% dispersion in water	<b>641855</b>
		Samarium strontium (50:50) cobalt oxide, 99.9%	<100	nanopowder	<b>677442</b>
63	<b>Eu</b>	Europium oxide 99.5%	60-100	nanopowder	<b>634298</b>
64	<b>Gd</b>	Gadolinium oxide 99.9+%	40-60	nanopowder	<b>637335</b>
		Gadolinium(III) oxide >99.9%	<80	5% dispersion in water	<b>641871</b>
65	<b>Tb</b>	Terbium oxide 99.5%	60-100	nanopowder	<b>634255</b>
66	<b>Dy</b>	Dysprosium oxide 99.9+%	60-100	nanopowder	<b>637289</b>
		Dysprosium(III) oxide >99.9%	<80	5% dispersion in water	<b>639664</b>
67	<b>Ho</b>	Holmium(III) oxide 99.9+%	40-60	nanopowder	<b>637327</b>
		Holmium(III) oxide >99.9%	<80	5% dispersion in water	<b>641863</b>
68	<b>Er</b>	Erbium oxide 99.9+%	40-60	nanopowder	<b>637343</b>
		Erbium(III) oxide	<80	5% dispersion in water	<b>641839</b>
70	<b>Yb</b>	Ytterbium oxide 99.7+%	40-60	nanopowder	<b>637300</b>
73	<b>Ta</b>	Tantalum 99+%	100	nanopowder	<b>593486</b>
74	<b>W</b>	Tungsten, activated 99.9+%	100	nanopowder	<b>577294</b>
		Tungsten(VI) oxide	35-40	nanopowder	<b>550086</b>
78	<b>Pt</b>	Platinum, activated 99.9+%	~100	nanopowder	<b>483966</b>
79	<b>Au</b>	Gold 99.9+%	50-130	nanopowder	<b>636347</b>
		Gold colloid	17-23	approx. 0.01% HAuCl <sub>4</sub> in water	<b>G1652</b>
		Gold colloid	3.5-6.5	approx. 0.01% HAuCl <sub>4</sub> in water	<b>G1402</b>
		Gold colloid	8.5-12.0	approx. 0.01% HAuCl <sub>4</sub> in water	<b>G1527</b>
		Gold colloidal	3-6	0.01% HAuCl <sub>4</sub> in toluene	<b>54349</b>
		Dodecanethiol functionalized gold nanoparticles	4-5	2% dispersion in toluene	<b>660434</b>
		Octanethiol functionalized gold nanoparticles	~3	2% dispersion in toluene	<b>660426</b>
83	<b>Bi</b>	Bismuth(III) oxide 99.9+%	90-120	nanopowder	<b>637017</b>
		Bismuth cobalt zinc oxide 99.9%	60-100	nanopowder	<b>631930</b>

For package size and prices, please visit [sigma-aldrich.com](http://sigma-aldrich.com).

For questions, product data, or new product suggestions,  
please contact the Materials Science team at [matsci@sial.com](mailto:matsci@sial.com).

## Quantum Dots: An Emerging Class Of Soluble Optical Nanomaterials



Professor Philippe Guyot-Sionnest,  
Depts. of Physics, Chemistry and  
The James Franck Institute,  
University of Chicago

Colloidal Quantum Dots (QDs) offer a striking visual demonstration of Quantum Mechanics. Atomic structures and sizes of the QD nanocrystals can be clearly seen in electron micrographs. When illuminated by an ultraviolet light, the nanocrystal solutions glow in vibrant and distinct colors. It is impressive to see the direct correspondence between the colors, from red to blue, and the increasing sizes of the nanoparticles (**Figure 1**). This compelling demonstration of Quantum Mechanics is the result of many years of advances in synthetic colloidal chemistry, motivated by developing technological interest in QD materials. This article will highlight the convergence of physics, chemistry, and materials science that made this emerging class of materials possible.

### QD Physics

An electron confined in a potential energy box is the most elementary problem we tackle when first exposed to quantum mechanics. We learn that the electron kinetic energy increases as the box gets smaller. This is the result of the uncertainty relation  $\Delta x \Delta p \geq \hbar/2$ , one of the fundamental principles of quantum mechanics. Using a box length  $L = \Delta x$  and electron momentum  $p = mv$ , the minimum kinetic energy of the electron is no longer zero but a finite value  $E = \hbar^2/2mL^2$  (with Planck's constant  $\hbar$  and electron mass  $m$ ). This expression is the basic principle behind the effect of size  $L$  on the color of semiconductor quantum dots. In addition, the defining property of a semiconductor is that there is an energy gap (band-gap) between a filled continuum of electron energy states (valence band) and an empty continuum of states (conduction band). A nanocrystal is a small semiconductor box and therefore the band-gap between the valence state and the empty state increases as the box gets smaller (**Figure 2**).

The above expression, which uses the free electron mass  $m$ , predicts very small effect of box size on the semiconductor band-gap at the nm scale. The problem is the use of the free electron mass. In crystalline solids, electrons behave as quantum mechanical waves, "sneaking through all the ions" as Felix Bloch put it, so that instead of the free electron mass  $m$ , they behave as if they had an "effective mass"  $m^*$ .<sup>1</sup> These effective masses were measured by cyclotron resonance starting in the mid-1940s. In some semiconductor materials, the effective masses can be quite small, a tenth or a hundredth of the free electron mass. For example, for CdSe, the effective mass is 0.13 the free electron mass. The smaller mass makes the semiconductor materials much more sensitive to the size of the box at the nm scale, and this has dramatic consequences, the most obvious being the increasing energy gap for smaller nanocrystals.

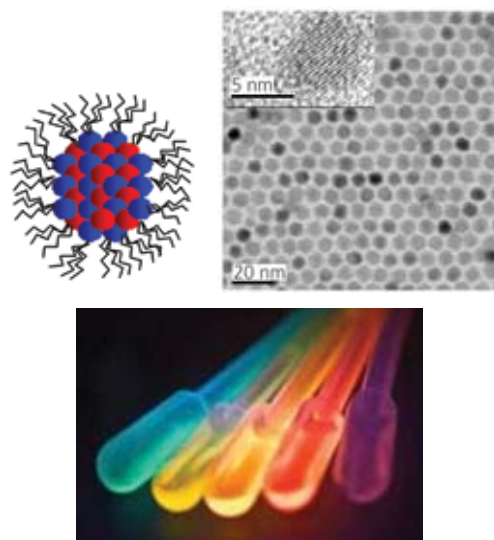


**Figure 1.** Top panel: Schematic image (left) of a QD nanocrystal core surrounded by solubilizing ligands; TEM image (right) of a dried film of monodisperse QDs packed in a hexagonal array. A high-resolution picture of a single QD showing atomic planes is shown in the inset. Bottom Panel: Fluorescence display of colloidal solutions of CdSe/ZnS Quantum Dots.

The particle in the box concept applied to semiconductors first surfaced in the 1960's at IBM.<sup>2</sup> Molecular Beam Epitaxy allowed building thin layers of materials with atomic precision thickness, such as GaAs/Al<sub>x</sub>Ga<sub>1-x</sub>As heterostructures. These one-dimensional electron boxes were called Quantum Wells. One purpose of that work was to "engineer" the lowest energy transitions of semiconductors by choosing the well size. Another consequence of the spatial confinement is to increase the probability of recombination of an electron in the conduction band and a missing electron (hole) in the valence band. This makes Quantum Wells excellent tunable diode lasers. Today, most semiconductor lasers used in optical communications and optical data storage systems (such as DVDs) are based on Quantum Well heterostructures.

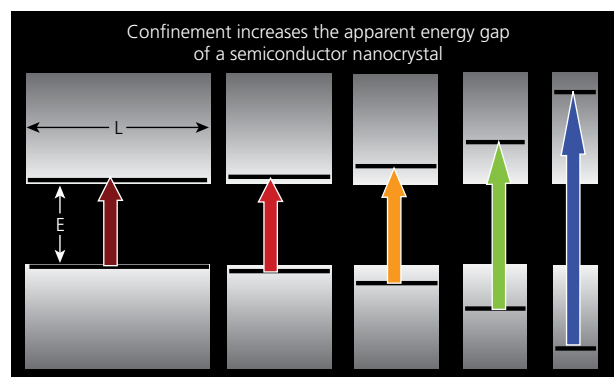


**Figure 2.** Schematic of the effect of the decreased size of the box on the increased energy gap of a semiconductor quantum dot, and the resultant luminescent color change from bulk materials (left) to small nanocrystals (right).

## QD Chemistry

Quantum Dots extend the idea of quantum confinement to three dimensions, and colloidal chemistry is a very natural way to make nanoscale semiconductor particles. The topic originated in the early 80's, when papers in the Russian literature discussed the size-dependent absorption spectra of colloidal semiconductor nanocrystals grown in molten transparent glasses or crystals.<sup>3,4</sup> Fast-forward in time, and we have colorful luminescent solutions of QD colloids, covering the near UV to near IR, which can be purchased from a growing number of companies around the world.

This achievement arose from many synthetic advances over the past twenty years. At first, the chemistry community explored colloidal semiconductor nanocrystals synthesized by aqueous and ionic chemistry. Part of the motivation, following the first oil crisis, was the development of nanocrystals for solar energy conversion and photocatalysis. Besides using quantum confinement to optimally tune the absorption wavelength and redox potential of the nanocrystals, it was felt that the high surface area of the particles would improve collection efficiency or surface reaction yields.<sup>5,6,7</sup> However, the aqueous colloidal synthesis made materials with poor size distribution and low fluorescence efficiency. While monodispersed colloidal growth was well known for amorphous sub- $\mu\text{m}$  sulfur or silica particles, as in the earlier works of La Mer<sup>8</sup> or Stauber,<sup>9</sup> the growth of crystalline monodispersed nm-sized colloids turned out to be more difficult. Further improvements in material properties waited for the development of a better synthetic approach.

In 1993, new scientific breakthroughs radically shifted the synthesis of semiconductor nanocrystals toward using high-temperature organic solvents. With pyrophoric metal-organic complexes that rapidly decompose, and long chain surface-passivating ligands, it became possible to achieve fast nucleation and slow growth of the nanocrystals, while maintaining a high enough temperature to anneal defects.<sup>10</sup> This resulted in vastly improved crystalline nanoparticles with high monodispersity and strong confinement. These new materials, at first mostly CdSe, led to many advances in the characterization of the electronic properties of the colloidal Quantum Dots (**Figure 3**). Using this route, colloidal quantum dots of other materials, for example II-VI and III-V semiconductors, could also be synthesized.

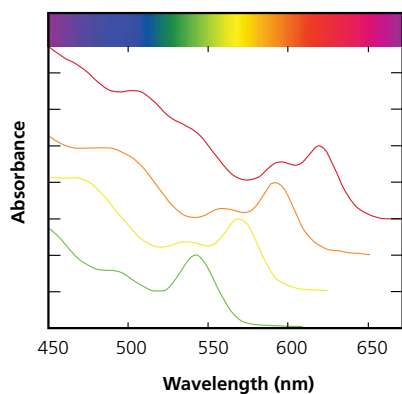


**Figure 3.** Absorption spectra of four CdSe colloidal quantum dots with distinct diameters from 3.5 nm to 5 nm. The synthesis with cadmium acetate and selenium requires no glove box and produces quality nanocrystals without post-reaction processing. Bulk CdSe is gray and absorbs below 720nm. The structure in the spectra is due to optical transitions between discrete (quantized) energy states within the valence and conduction bands of the nanocrystals.

An important feature of the small nanocrystals is the great proportion of surface atoms. If the goal is to achieve a good and stable luminescence yield, the surface must be inert to the excited electrons. In other words, there can be no surface states to trap the electron. Materials with a simple CdSe core had poor photoluminescence and moderate photostability. In 1996, this drawback was solved by growing a shell of ZnS,<sup>11</sup> a higher band gap semiconductor, around the CdSe core. The CdSe/ZnS core/shell Quantum Dots, and subsequent core/shell systems afforded strong and sturdy photoluminescence which further generated interest for these materials. Still, the use of pyrophoric metal organic precursors was a major inconvenience. In 2000, the introduction of stable ionic precursors, or "green" precursors,<sup>12</sup> dramatically reduced the psychological barrier and some of the potential hazards of the synthesis of II-VI nanoparticles. This was achieved without losing any of the unique physical properties of materials prepared by earlier synthetic methods, as shown in Figure 3. This approach, since then demonstrated for many II-VI and IV-VI semiconductors, has led to an explosion in the number of groups synthesizing and investigating semiconductor nanocrystals. The new methods to synthesize the nanoscale colloids, coupled with visualization by Transmission Electron Microscopy (TEM), are now facilitating serendipitous discoveries of materials with novel shapes. The last five years produced about 5 times more scientific publications on colloidal quantum dots than the previous twenty years combined. What has sustained the growth of research activity is the potential of these novel colloidal materials for improving existing technologies or developing novel applications.

## QD Applications

To date, the most successful application is the use of colloidal Quantum Dots as biological tags, a strategy first demonstrated in 1998.<sup>13,14</sup> It turns out that core/shell Quantum Dots can be made more photostable (long-lived) than existing molecular dyes. They also exhibit narrower luminescence, a broader and continuous absorption spectrum, and can be tuned to the near infrared with still high quantum efficiency. For all these excellent reasons, there is a considerable level of activity to modify the surface of the Quantum Dots, rendering them specific for imaging particular biological targets.

A more traditional area of application of semiconductors is electro-optic devices, such as Light-Emitting Diodes (LEDs), Photovoltaics (PV), and lasers. The colloidal nature of Quantum Dots opens up the route to cheap and large-scale processing of semiconductor thin films using spraying or printing methods. The challenge is to combine their good optical properties with equally good electronic properties. Great progress is being made. For example, a few years after the inception of Organic LEDs, it was suggested that Quantum Dots could also be used to make LEDs<sup>15</sup> with similar potential benefits for large area and flat panel displays. Recently, LEDs with efficiencies of a few percent, sufficient for commercial interest, have been achieved.<sup>16</sup>

For questions, product data, or new product suggestions,  
please contact the Materials Science team at [matsci@sial.com](mailto:matsci@sial.com).

Another possible application of Quantum Dots, highlighted by recent energy concerns, is in solar energy conversion. This was one of the early motivations for these materials and is again actively researched by many groups. To print large area solar cells, semiconductor colloids are a valid starting point. It is also a possibility that the “Quantum Dot” nature of the material may be an advantage. Selecting particle sizes would allow optimal tuning of the absorption band gap to match the solar spectrum, and it is also believed that it might help to extract the energy from short wavelength photons.<sup>17</sup>

There are other promising applications presently pursued with lesser vigor such as using colloidal Quantum Dots to make semiconductor lasers. Quantum Dots have long been proposed as the best semiconductor materials for highly efficient lasers,<sup>18</sup> and Molecular Beam Epitaxy has been used to make electrically driven heterostructure Quantum Dot lasers for nearly a decade. However, the colloidal Quantum Dot packing density achieved so far in these devices is too low to provide a net advantage over existing Quantum Well lasers. With dried films of close-packed colloidal Quantum Dots (Figure 1), the packing density can be increased significantly showing great promise for improved lasers. At present, photo-pumped lasing has been demonstrated,<sup>19</sup> and electrically pumped lasing is a challenge for the future. Another possible display application, with low current requirements, would use the color changes of redox-active Quantum Dots. Adding two electrons to a Quantum Dot fills the lowest unoccupied energy state in the conduction band, which changes the absorption of the dot, thereby changing its color.<sup>20</sup> This flexibility of changing Quantum Dot colors, by engineering their redox potentials, makes this application possible.

Colloidal Quantum Dots have a particular niche as optical materials in the infrared. Indeed, in the visible and UV spectral range, organic dye molecules can have near 100% photoluminescence efficiency and Quantum Dots struggle to compete. However, in the near-infrared QDs win easily. This is because organic dye molecules have high frequency vibrations that couple strongly with electronic transitions. Thus the quantum yield of dye molecules falls below 1% at wavelengths around 1  $\mu\text{m}$  and organic dyes provide no detectable photoluminescence beyond 2  $\mu\text{m}$ . Inorganic Quantum Dots made from semiconductor materials with heavy atoms and infrared band gaps have very low vibrational frequencies and some, such as PbSe, can be excellent emitters in the near infrared. Quantum Dots can be strong emitters in the mid-infrared as well, and there has been progress in this direction in recent years.<sup>21</sup> Potential applications could include earth to satellite communications through the atmosphere transparent bands with wavelengths of 3-5  $\mu\text{m}$  and 8-10  $\mu\text{m}$ .

There are many interesting chemical challenges to further applications of colloidal Quantum Dots. Besides size, shape, and surface control, semiconductor composition is an issue. For example, doping n- or p-type impurities in Quantum Dots is important for electronic applications. Adding magnetic impurities inside a small nanocrystal is a way to strongly enhance the magnetic response of the nanocrystals.<sup>22</sup> Research is intense in this direction, with the goal being to make new magneto-optic and spintronic materials. It is clear that colloidal Quantum Dots have a bright future as specialty optical materials. They are one example of a general trend toward rational design of nanomaterials where known principles of physics are fused with modern chemical techniques to create nm-sized materials with properties optimized for targeted applications.

## References

- (1) Charles Kittel, *Introduction to Solid State Physics*, 8th edition, **2005**, Wiley.
- (2) Esaki, L., and Tsu, R., *IBM J. Res. Develop.*, **1970**, *14*, 61; Chang, L.L., Esaki, L., *Phys. Today*, **1992**, *45*, 36.
- (3) Ekimov, A.I., Onushchenko, A.A., *JETP Lett.*, **1981**, *34*, 345.
- (4) Efros, A.L., Efros, A.L., *Soviet Phys. Semiconductors-USSR*, **1982**, *16*, 772.
- (5) Brus, L.E., *J. Chem. Phys.*, **1983**, *79*, 5566.
- (6) Henglein, A., *Chem. Rev.*, **1989**, *89*, 1861.
- (7) Kamat, P.V., *Chem. Rev.*, **1993**, *93*, 267.
- (8) LaMer, V.K., Dinegar, R.H., *J. Am. Chem. Soc.*, **1950**, *72*, 4847.
- (9) Stober, W., Fink, A., Bohn, E., *J. Coll. Interf. Science*, **1968**, *26*, 62.
- (10) Murray, C.B., Norris, D.J., Bawendi, M.G., *J. Am. Chem. Soc.*, **1993**, *115*, 8706.
- (11) Hines, M.A., Guyot-Sionnest, P., *J. Phys. Chem.* **1996**, *100*, 468.
- (12) Peng, Z.A., Peng, X.G., *J. Am. Chem. Soc.*, **2001**, *123*, 183.
- (13) Bruchez, M., Moronne, M., Gin, P., Weiss, S., Alivisatos, A.P., *Science*, **1998**, *281*, 2013.
- (14) Chan, W.C.W., Nie, S.M., *Science*, **1998**, *281*, 2016.
- (15) Colvin, V.L., Schlamp, M.C., Alivisatos, A.P., *Nature*, **1994**, *370*, 354.
- (16) Coe S., S., Woo, W.K., Bawendi, M., Bulovic, V., *Nature*, **2002**, *420*, 800.
- (17) Nozik, A.J., *Physica E-Low Dim. Sys. & Nano.*, **2002**, *14*, 115.
- (18) Arakawa, Y., Sakaki, H., *Appl. Phys. Lett.*, **1982**, *40*, 939.
- (19) Klimov, V.I., Mikhailovsky, A.A., Xu, S., Malko, A., Hollingsworth, J.A., Leatherdale, C.A., Eisler, H.J., and Bawendi, M.G., *Science*, **2000**, *290*, 314.
- (20) Shim, M., Guyot-Sionnest, P., *Nature*, **2000**, *407*, 981.
- (21) Pietryga, J.M., Schaller, R.D., Werder, D., Stewart, M.H., Klimov, V.I., Hollingsworth, J.A., *J. Am. Chem. Soc.*, **2004**, *126*, 11752.
- (22) Norris, D.J., Yao, N., Charnock, F.T., Kennedy, T.A., *Nano Lett.*, **2001**, *1*, 3.

## It's Here! NEW Aldrich Handbook



- ✓ 35,000 Material Listings
- ✓ 2,000 NEW Products
- ✓ 6,100 Citations
- ✓ 3,000 Application Notes
- ✓ Enhanced Application Index
- ✓ Advanced Product Tables

Reserve your  
FREE set today.

Visit  
[sigma-aldrich.com/handbook35](http://sigma-aldrich.com/handbook35)

RESEARCH IS EASIER WHEN  
YOU USE THE RIGHT TOOLS!

**Aldrich Handbook of Fine Chemicals**  
Enhanced Application Index includes Materials Science.

### Featuring:

- Chemical Solution Deposition/Sol-Gel Processing
- Chemical Vapor Deposition
- Conducting Polymers
- Fuel Cells
  - Materials for Hydrogen Storage
  - Proton Exchange Membrane (PEM) Material
- Nanoparticles
  - Nanopowders & Nanodispersions
  - Functionalized Nanoparticles
  - Quantum Dots
- Electronic Grade Materials



Set Includes the  
**NEW**  
Sigma-Aldrich  
Labware Catalog

Catalog Cover: The Alchemist (ca. 1937) by Newell Conover Wyeth. Courtesy of the Chemical Heritage Foundation Image Archives.

TO ORDER: Contact your local Sigma-Aldrich office (see back cover),  
call 1-800-325-3010 (USA), or visit [sigma-aldrich.com/matsci](http://sigma-aldrich.com/matsci).

## The Application of Quantum Dots in Display Technology



Dr. Seth Coe-Sullivan  
Co-Founder and CTO, QD Vision, Inc.

Quantum Dots (QDs), a nanoscale material with unique optical properties governed by quantum mechanics, have been incorporated into a new display technology under development at QD Vision, Inc. QDs are nanoscale colloidal semiconductors with bandgaps tunable by the size of the colloid. QD Vision combines these materials with organic molecules and processing techniques of plastic electronics to create a new class of solid-state displays. Organic materials are promising materials for light-emitting devices, including displays, because they can be made inexpensively, can be deposited on flexible substrates, and shine brightly. But an even better device could result if the benefits of organic materials were combined with the unique properties of Quantum Dots. While proof of concept QD-LEDs had been made before, these early devices were several orders of magnitude lower in efficiency and brightness than was necessary for a commercially viable device technology. QD Vision's founders developed new fabrication methods, such as the technique of phase separation<sup>1</sup> that allowed QD-LEDs with record efficiencies to be made from QDs and small molecule organic transport materials (such as Alq<sub>3</sub> and TPD<sup>2</sup> as opposed to the polymers used in previous work).

In many ways, QDs are an ideal lumophore for incorporation into LEDs for large area flat panel displays (FPD). QD emission can be tuned continuously through large portions of the

electromagnetic spectrum. For example, CdSe Quantum Dots can emit from 470 nm to 640 nm light, almost the entire visible spectrum (**Figure 1**). Because their emission can be tuned throughout the visible spectrum, they can become the only lumophore that is necessary in a full color flat panel display. Furthermore, QDs have a unique combination of performance attributes not achievable with other lumophores. The ideal OLED lumophore would have high photoluminescence quantum yield, be capable of emitting light from 100% of electrically generated excitons, be solution processable, and have extremely high stability and differential stability (when compared to different color lumophores of the same class). Polymers, dendrimers, fluorescent small molecules and phosphorescent small molecules have all undergone extensive development, but have yet to yield a single material set that meets the complete set of industry needs. Quantum Dots are a new class of lumophores that have the promise to meet all these needs simultaneously.

QDs also have the potential to allow efficient manufacturing, as they are compatible with solution thin-film deposition techniques, e.g., spin-casting, Langmuir-Blodgett, or drop-casting. Such techniques can be applied to additive processing, and hence can save costly steps in display fabrication. However, these methods place requirements on the substrate onto which the QDs are deposited, do not allow the QD layer to be laterally patterned, and are largely incompatible with the small molecule, transport layer materials that comprise the rest of a hybrid device. These difficulties can be circumvented by the technique of QD contact printing. This dry deposition technique for QD solids ensures that no solvent, or other impurities, would ever contact the device substrate during device fabrication, and allow for the additive, patterned deposition of QDs. Thus, a single step QD deposition process that is high speed, high throughput, and high yield can be envisioned, greatly reducing FPD fabrication costs.

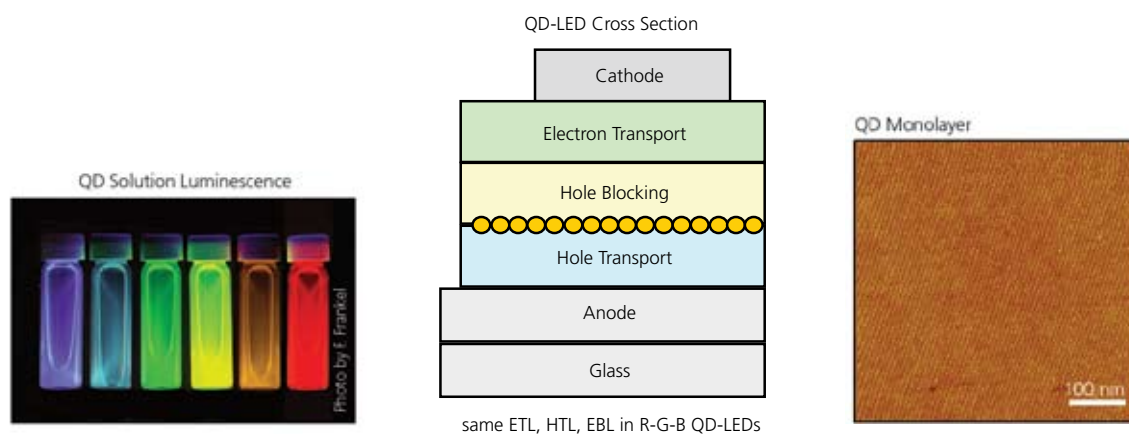


**Figure 1.** Left: Vials of fluorescent CdSe QDs dispersed in hexane showing the effect of quantum confinement. QD sizes range from 2 nm (blue) to 8 nm (red) from left to right. CdSe is one example of a QD material that can be used with our device architecture shown in cross-section (Center). The device utilizes only a monolayer of QDs, allowing saturated QD Color emission, while keeping the operating voltage of the device low. Right: AFM micrograph of PbSe QD monolayer showing the nanoscale morphology of the QD monolayer within an infrared emitting device, useful for a wide range of military and communications applications.

For questions, product data, or new product suggestions,  
please contact the Materials Science team at [matsci@sial.com](mailto:matsci@sial.com).

A prototype display that demonstrates the visual appeal of QD Vision's QD-LED technology is shown in **Figure 2**. A 64 x 32 pixel monochrome passive matrix display with a 1.4" diagonal dimension emitting in vivid red and green colors have already been developed. The form factor is that of a cell phone display, and its ultrathin 1.5 mm (<1/16<sup>th</sup> of an inch) profile lends itself to the slim format phones popular today.



**Figure 2.** Photograph of QD Vision's prototype QD Display. The prototype is fabricated using the contact printing technique, resulting in high levels of uniformity over a 1.4" diagonal screen.

QD-LEDs have theoretical performance limits that meet or exceed all other display technologies. Phosphorescent OLEDs have the best-demonstrated efficiency of any non-reflective display technology, but QD-LEDs have the potential to exceed their luminous efficiency by over 20%, reducing power consumption significantly. The narrow emission spectra of QDs result in an extremely wide color gamut, and thus QD displays have the potential for color saturation better than both LCD and OLED displays. As an inorganic emitting body, they are far more stable than most organic emissive materials. QD-LEDs offer the combination of high brightness and efficiency with long lifetime, hence differentiating itself from LCDs, OLEDs, and plasma displays alike.

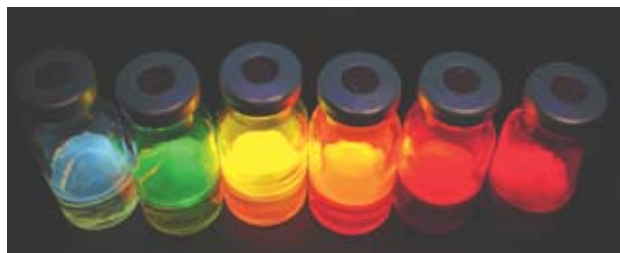
#### References:

- (1). Coe-Sullivan, S., Steckel, J.S., Woo, W.K., Bawendi, M.G., Bulovic, V., *Adv. Funct. Mater.*, **2005**, *15*, 1117. (2). Alq<sub>3</sub> tris-(8-hydroxyquinoline) aluminum, and *N, N'*-diphenyl-*N, N'*-bis(3-methylphenyl)-(1,1'-biphenyl)-4,4'-diamine, respectively.

Novel applications of QDs are made possible by improvements in QD materials, as well as availability of materials that make QDs work in applications such as QD-LEDs. To help our customers do innovative research, Sigma-Aldrich offers a broad range of inorganic as well as organic materials for next-generation plastic electronics. Available materials include electron-transporters (e.g. Alq<sub>3</sub>, **444561**), hole-transporters (e.g., TPD, **443263**), and ITO substrates (e.g., **636916**).

For a complete list, please visit [sigma-aldrich.com/organicelectronics](http://sigma-aldrich.com/organicelectronics).

For more information on organic electronic materials visit [sigma-aldrich.com/mslit](http://sigma-aldrich.com/mslit) to download *ChemFiles Vol. 5, No. 8, Organic Electronic Materials* and *ChemFiles Vol. 4, No. 6, Organic Semiconductors for Advanced Electronics*.



## Quantum Dots from Sigma-Aldrich

Quantum Dot Type	Quantum Dot Material System	Concentration	Emission Peak (nm)	Measured Emission Range (nm)	FWHM (nm)	Size* (nm)	Extinction Coefficient (10 <sup>5</sup> cm <sup>-1</sup> M <sup>-1</sup> )	Quantum Yield**	Prod. No.
Core	<b>Lumidot™ CdS-6 Kit</b>								<b>662593</b>
	CdS 360	Dispersion (25 mg in 5 mL toluene)	360	367 - 386	20	1.6-1.8	2.0	~50%	
	CdS 380	Dispersion (25 mg in 5 mL toluene)	380	387 - 406	18	1.8-2.3	2.7	~50%	
	CdS 400	Dispersion (25 mg in 5 mL toluene)	400	407 - 425	18	2.3-2.9	2.7	~50%	
	CdS 420	Dispersion (25 mg in 5 mL toluene)	420	426 - 444	20	2.9-4.0	6.8	~50%	
	CdS 440	Dispersion (25 mg in 5 mL toluene)	440	445 - 462	18	4.0-5.4	10.2	~50%	
	CdS 460	Dispersion (25 mg in 5 mL toluene)	460	463 - 482	20	5.4-7.3	2.7	~50%	
Core	<b>Lumidot™ CdSe-6 Kit</b>								<b>662550</b>
	CdSe 480	Dispersion (25 mg in 5 mL toluene)	480	481 - 502	24	2.1-2.3	0.49	~50%	
	CdSe 520	Dispersion (25 mg in 5 mL toluene)	520	525 - 542	25	2.4-2.6	0.68	~50%	
	CdSe 560	Dispersion (25 mg in 5 mL toluene)	560	563 - 572	25	3.0-3.5	1.2	~50%	
	CdSe 590	Dispersion (25 mg in 5 mL toluene)	590	595 - 611	24	4.0-4.3	2.5	~50%	
	CdSe 610	Dispersion (25 mg in 5 mL toluene)	610	518 - 627	25	4.7-5.2	3.7	~50%	
	CdSe 640	Dispersion (25 mg in 5 mL toluene)	640	639 - 653	24	6.2-7.7	8.6	~50%	

TO ORDER: Contact your local Sigma-Aldrich office (see back cover), call 1-800-325-3010 (USA), or visit [sigma-aldrich.com/matsci](http://sigma-aldrich.com/matsci).

Quantum Dot Type	Quantum Dot Material System	Physical form	Emission Peak (nm)	Measured Emission Range (nm)	FWHM (nm)	Size* (nm)	Prod. No.
Core-Shell	Lumidot™ CdSe/ZnS	Nanopowder	553	545 - 555	36	2.5	<b>53241</b>
Core-Shell	Lumidot™ CdSe/ZnS	Nanopowder	562	560 - 570	35	2.6	<b>69346</b>
Core-Shell	Lumidot™ CdSe/ZnS	Nanopowder	582	575 - 585	32	3.2	<b>30491</b>
Core-Shell	Lumidot™ CdSe/ZnS	Nanopowder	593	590 - 600	37	3.5	<b>53817</b>
Core-Shell	Lumidot™ CdSe/ZnS	Nanopowder	606	605 - 615	33	4.0	<b>97062</b>
Core-Shell	Lumidot™ CdSe/ZnS	Nanopowder	626	620 - 630	42	5.5	<b>63616</b>

Lumidot is a trademark of Sigma-Aldrich Corporation.

\* Particle size was determined by TEM according to the procedure in Yu, W.W., Qu, L., Guo, W., Peng, X., *Chem. Mater.*, **2003**, *15*, 2854.

\*\* Quantum yield was measured following the procedure of Qu, L., Peng, X., *J. Am. Chem. Soc.*, **2002**, *124*, 2049.

Low-cost processing of multi-layered circuits and devices is a potential advantage of plastic and nanomaterial-based electronics. Substrate preparation and film deposition from solution are two key steps in the fabrication of these devices. To give our customers the tools to do such work, Sigma-Aldrich offers reliable and simple-to-use instruments, including Plasma Cleaners and Spin-Coaters.

### Tabletop Plasma Cleaners

An inductively coupled plasma device used for surface cleaning, preparation and modification. Plasma treatment may be applied to a wide variety of materials.

Basic model has a removable cover. Applies a maximum of 18W to the RF coil, with no RF emission.

Prod. No.	Description
<b>Z561673</b>	110V US plug
<b>Z561681</b>	220V European plug

Expanded design has hinged cover with viewing window and integral switch for a vacuum pump. Applies a maximum of 30W to the RF coil with no RF emission.

Prod. No.	Description
<b>Z561657</b>	110V US plug
<b>Z561665</b>	220V European plug



#### Useful for:

- surface sterilization
- activation
- energy alteration
- surface preparation for bonding and adhesion
- surface treatment of polymers and biomaterials

#### Features:

- Adjustable RF power
- Low, medium, and high power settings
- Optional flow mixer allows individually metered intakes for up to two different gases and monitors the chamber
- 1/8 in. NPT needle valve to admit gases and control the pressure
- Pyrex plasma cleaner chamber



### Chemat Spin Coater

Easy-to-use equipment for thin film fabrication by spin-coating. It provides a convenient step-by-step method for processing solutions. A two-stage spin process allows dispensing at low speeds and homogenizing the coating at high speeds.

Prod. No.	Description
<b>Z551562</b>	110V US plug
<b>Z551589</b>	220V European plug
<b>Z558508</b>	Programmable

For questions, product data, or new product suggestions, please contact the Materials Science team at [matsci@sial.com](mailto:matsci@sial.com).

## En Route to Carbon Nanotube Electronics



Professor Moonsub Shim  
Department of Materials Science and  
Engineering and Frederick Seitz Materials  
Research Laboratory, University of Illinois  
at Urbana-Champaign

Ballistic electron transport, current carrying capacities on the order of  $10^9$  A/cm<sup>2</sup>, and one of the largest known specific stiffness are only a handful of the many exciting and potentially useful properties of single-walled carbon nanotubes (SWNTs).<sup>1</sup> Especially in developing areas of electronics such as wearable/flexible electronics and nanoelectromechanical systems, SWNTs may find use as high performance semiconducting as well as conducting elements. However, as with any new material, there are many obstacles to overcome before most envisioned benefits can be realized. Three of the biggest challenges to be addressed in order to integrate SWNTs into high performance electronic devices are; 1) electronic inhomogeneity where a random mixture of metallic and semiconducting SWNTs can degrade device performance, 2) extreme sensitivity to minute changes in the local chemical environment, and, 3) difficulties in aligning and patterning. While the first challenge is specific to SWNTs, the second and the third issues are general to one-dimensional materials. Here, we briefly discuss some of our current efforts in addressing all three challenges.

### Electronic Inhomogeneity

The distribution of diameters and chirality in SWNTs produced by current synthetic methods leads to a mixture of metallic and semiconducting characteristics. This electronic inhomogeneity imposes one of the biggest challenges in all prospects for electronic implementations. One obvious but devastating consequence of the electronic inhomogeneity in developing high performance transistors out of SWNTs is that metallic SWNTs will electrically short the semiconducting channels. This appears as a large off-current in the transport characteristics of transistors composed of multiple SWNTs as shown in the uppermost curve in **Figure 1A**. Recently demonstrated selective chemical functionalization methods may provide a simple scalable means of eliminating metallic tubes from SWNT transistors and electronic devices. We have carried out a combination of electron transport and Raman studies on the reaction of 4-bromobenzene diazonium tetrafluoroborate (4-BBDT, **Aldrich 673405**) directly with single and networks of SWNT transistors to examine the potential benefits and limitations of this approach.<sup>2</sup>

Figure 1A shows the electrical response of a transistor consisting of multiple SWNTs (both metallic and semiconducting) upon reaction with increasing concentration of 4-BBDT. The best case scenario where only metallic SWNTs react and become insulating is achieved at 5  $\mu$ M. At this concentration, the reduction in the off-current is essentially identical to the decrease in the on-current indicating that only the metallic SWNTs which do not have gate voltage dependent drain-source current have reacted. The key result is that the performance in terms of carrier mobility remains the same when only the metallic SWNTs are chemically turned off.

**Figure 1B** shows the ratio of intensities of disorder (D) and tangential G (in-plane C-C stretch) Raman modes of several SWNTs upon reaction with 4-BBDT of increasing concentration. The D mode arises from a double resonance process where momentum conservation is achieved by defect (or disorder) scattering. Since 4-BBDT reacts with SWNTs by covalent C-C bond formation, it inevitably breaks pi-bonds of SWNTs. This chemical reaction then induces additional disorder leading to the enhancement of D mode in the Raman spectra of SWNTs. Hence the ratio of intensities of D and G modes provides a simple spectroscopic measure of chemical reactivity. The metallic SWNTs are found to have, on average, higher reactivity towards 4-BBDT. However, there is a considerable overlap between metallic and semiconducting SWNTs. While in a device consisting of a limited number of SWNTs, the ideal situation of selectively turning off metallic SWNTs can be achieved, when there is a large number of SWNTs, a significant degradation of device performance is inevitable and is observed. While reaction with 4-BBDT cannot be applied directly to improve device performance beyond transistors consisting of a limited number of SWNTs, additional factors such as external electrochemical potential to shift the Fermi levels of SWNTs may be exploited to achieve improvements and are being examined.

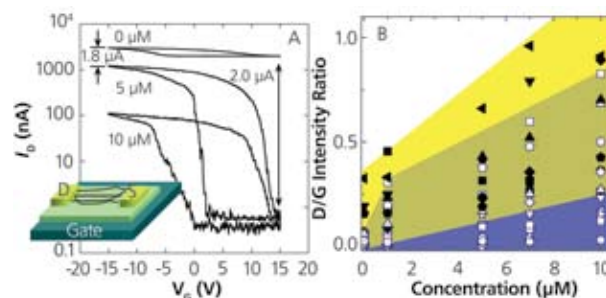


**Figure 1.** A. The electrical response of SWNTs which are the active elements within a back-gated transistor (schematic) upon reaction with 4-bromobenzene diazonium tetrafluoroborate (4-BBDT) of indicated concentrations. B. Reactivity distribution of metallic and semiconducting SWNTs to 4-BBDT as measured by the increasing disorder (D) to tangential (G) band intensity ratio in the Raman spectra. Filled symbols – metallic; Open symbols – semiconducting.

## Extreme Sensitivity to the Local Chemical Environment

Another key challenge in integrating SWNTs into electronics is the extreme sensitivity to molecular adsorption and to changes in the local chemical environment. Some consequences in terms of electronic applications include difficulties in achieving complementary p- and n-type devices (i.e. doping) due to oxygen adsorption<sup>3</sup> and large hysteresis<sup>4</sup> associated with interaction with the substrate. Extremely environment sensitive electronic properties of SWNTs can also lead to undesirable and/or unpredictable behavior even with small changes in the surrounding medium. All of these challenges can actually be overcome by exploiting the highly sensitive electronic properties of SWNTs. With simple adsorption of polymers having appropriate chemical groups, electron or hole injection can be achieved.<sup>5</sup> Addition of an electrolyte into the host polymer allows electrochemical gating with efficiencies approaching the ideal limit and eliminating hysteresis.<sup>6</sup> The short Debye lengths of the electrolyte solution can also screen out many undesirable external effects.

Device characteristics of individual SWNT transistors operating in the back gate configuration are shown in the insets of **Figure 2**. Notice that all devices show p-channel operation (negative gate voltages) with little or no n-channel conductivity and large hysteresis. The main panels of Figure 2 show the same corresponding SWNTs operating with polymer electrolyte gate. Within the gate voltage range examined, very low leakage current of < 500 pA at relatively large gate voltages and < 100 pA near depletion region (mainly due to non-Faradaic charging currents in electric double layer formation) preserves the high on-off ratio of  $\sim 10^5$ . More importantly, varying the chemical groups of the host polymer from electron donating to electron withdrawing can tune the doping levels in semiconducting SWNTs while maintaining high carrier mobilities.

Polymer electrolyte adsorption provides a simple air-stable means of doping SWNTs in addition to blocking out other external chemical sensitivity via short Debye lengths. However, electrochemical gating is limited in terms of device switching speed since it relies on ionic mobility. Nevertheless, operation speed of several hundreds of Hertz observed in these devices is already useful for simple display applications. Further studies are on-going to develop strategies for enhancing device switching speeds and therefore fully exploiting high carrier mobilities of SWNTs.

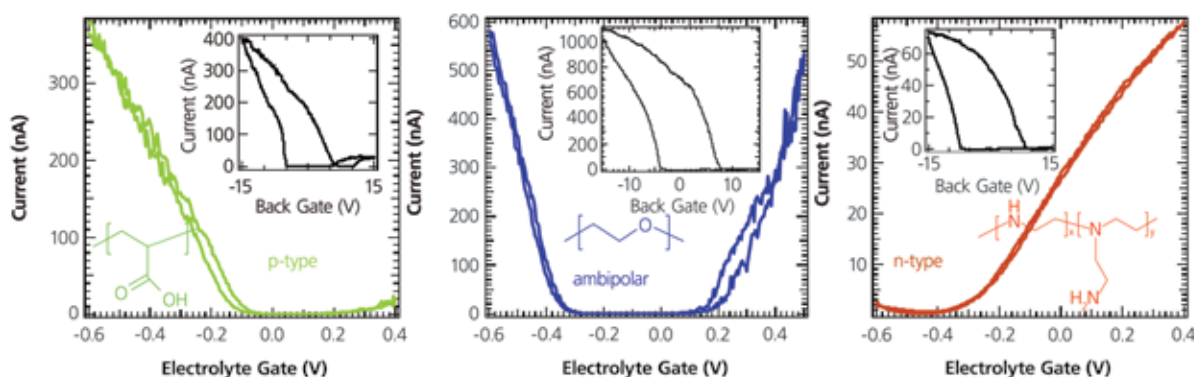


**Figure 2.** Carbon nanotubes gated with polymer electrolytes. Chemical groups of the adsorbed polymers can change initially p-type only devices (insets) into p-, n- and ambipolar devices. Polymers used are poly(acrylic acid) ( $M_n \sim 1240$ ) for p-type, poly(ethylene oxide) ( $M_n = 1000$ ) for ambipolar, and polyethylenimine ( $M_n \sim 800$ ) for n-type devices (see page 19 for a list of Sigma-Aldrich CNTs and polymers).

## Alignment and Patterning

The final challenge to be discussed here is the difficulties in aligning and patterning SWNTs. Vertical alignment in both multi-walled and single-walled carbon nanotubes have been achieved directly from chemical vapor deposition where the nanotubes grow out perpendicular to the substrate.<sup>7</sup> This geometry may be particularly useful for field emission applications. However, for many electronics applications, horizontal alignment along the substrate is desired. One solution involves exploiting interaction of SWNTs with the substrate. On mis-cut single crystal quartz, we have shown that SWNTs grow horizontally aligned along the quartz step edges.<sup>8</sup> **Figure 3A** shows a nearly perfect alignment of SWNTs grown on mis-cut quartz. By patterning catalyst particles (evaporated Fe or solution deposited Fe salts), interesting structures can be obtained as shown in **Figure 3B**. Where the catalysts are patterned, there is a very high density of SWNTs leading to random orientations. Away from the catalyst areas, SWNTs start to align along substrate step edges. The randomly oriented high density areas are highly conducting and can be used as the "electrodes" to contact the aligned SWNTs acting as the active elements in an all SWNT transistor.

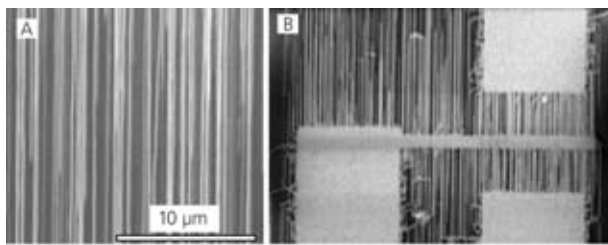


**Figure 3.** A. Nearly perfect horizontally aligned SWNTs directly grown on mis-cut single crystal quartz. B. An "all-SWNT transistor" where large density area on top of the patterned catalyst serves as conductors and the aligned SWNTs act as active elements.

## Conclusions

Advances in nanoelectronics continue to be anticipated from the exceptional properties of SWNTs. Most benefits may be gained in developing areas such as flexible electronics and nanoelectromechanical systems where an unprecedented combination of electrical and mechanical properties may be exploited together. We have addressed some of the major challenges to be overcome en route to integrating SWNTs into such devices and systems here.

## Acknowledgment

Contributions by C. Wang, G. Siddons, and C. Kocabas to this work and collaboration with Prof. J. Rogers are gratefully acknowledged. This material is based upon work supported by NSF (grant nos. DMR-0348585, CCF-0506660 and ECS-0403489).

## References

(1) (a) Javey, A., Guo, J., Wang, Q., Lundstrom, M., Dai, H., *Nature*, **2003**, 424, 654. (b) Yao, Z.; Kane, C.L.; Dekker, C., *Phys. Rev. Lett.*, **2000**, 84, 2941. (c) Baughman, R.H.; Zakhidov, A.A.; de Heer, W.A., *Science*, **2002**, 297, 787. (2) Wang, C.J., Cao, Q., Ozel, T., Gaur, A., Rogers, J.A., Shim, M., *J. Am. Chem. Soc.*, **2005**, 127, 11460. (3) (a)

Shim, M., Siddons, G.P., *Appl. Phys. Lett.*, **2003**, 83, 3564. (b) Shim, M., Back, J.H., Ozel, T., Kwon, K., *Phys. Rev. B*, **2005**, 71, 205411. (4) Kim, W., Javey, A., Vermesh, O., Wang, Q., Li, Y., Dai, H., *Nano Lett.*, **2003**, 3, 193. (5) Shim, M., Javey, A., Kam, N. W. S., Dai, H. J., *J. Am. Chem. Soc.* **2001**, 123, 11512. (6) (a) Siddons, G. P., Merchin, D., Back, J. H., Jeong, J. K., Shim, M., *Nano Lett.* **2004**, 4, 927. (b) Ozel, T., Gaur, A., Rogers, J. A., Shim, M., *Nano Lett.* **2005**, 5, 905. (7) (a) Li, W.Z., Xie, S.S., Qian, L.X., Chang, B.H., Zou, B.S., Zhou, W.Y., Zhao, R.A., Wang, G., *Science*, **1996**, 274, 1701. (b) Hata, K., Futaba, D.N., Mizuno, K., Namai, T., Yumura, M., Iijima, S., *Science*, **2004**, 306, 1362. (8) (a) Kocabas, C., Hur, S.H., Gaur, A., Meitl, M.A., Shim, M., Rogers, J.A., *Small*, **2005**, 1, 1110. (b) Kocabas, C., Shim, M., Rogers, J.A., *J. Am. Chem. Soc.*, **2006**, 128, 4540.

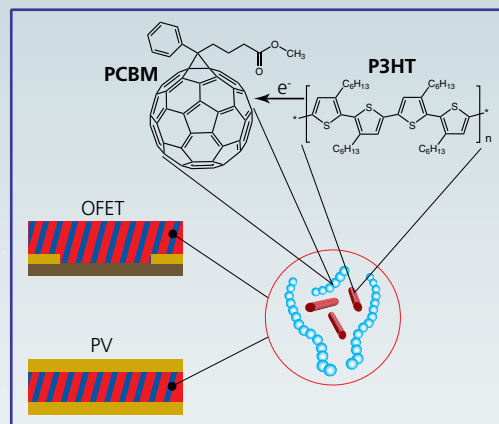
# Functionalized Fullerenes: Nanomaterials for Organic Electronics

Fullerenes, the older nanomaterial relatives of carbon nanotubes, continue to stimulate advances in applied and fundamental science. Fullerenes are excellent electron acceptors and can be chemically modified to improve solubility in organic solvents. Such soluble fullerenes are some of the best n-type organic semiconductors available to make bulk heterojunction photovoltaic cells (PVs)<sup>1,2</sup> and field-effects transistors (OFETs).<sup>3</sup> To help our customers achieve their research breakthroughs in organic electronics, Sigma-Aldrich is pleased to offer a line of functionalized fullerene products. Current products include PCBM (**659169**) and MP-C<sub>60</sub> (**668184**). PCBM is soluble in the same organic solvents as excellent p-type semiconductors (**Table 1**) and was recently used to make organic PVs with efficiencies ~4.4%.<sup>4</sup> MP-C<sub>60</sub> is another soluble electron acceptor often used as spectroscopic and redox reference for C<sub>60</sub>-donor conjugates.<sup>5,6</sup>

**Sigma-Aldrich is always looking to offer new products that will help you in your research. Please visit us at [sigma-aldrich.com/organicelectronics](http://sigma-aldrich.com/organicelectronics) for an up-to-date list of products, including new functionalized fullerenes.**

**Table 1:** Conduction (LUMO) and valence (HOMO) band energies of p- and n-type organic semiconductors available from Sigma-Aldrich.<sup>2,3</sup>

Organic semiconductor	Prod. No.	LUMO	HOMO	Soluble in:
MDMO-PPV p-type	<b>546461</b>	-2.8 eV	-5.0 eV	
MEH-PPV p-type	<b>541443</b> (MW 40 – 70 kDa)	-3.2 eV	-5.4 eV	chloroform chlorobenzene dichlorobenzene toluene
	<b>541435</b> (MW 70 – 100 kDa)			
	<b>536512</b> (MW 150 – 250 kDa)			
P3HT p-type	<b>445703</b> (regioregular)	-3.2 eV	-5.1 eV	
	<b>510823</b> (regiorandom)			
	<b>669067</b> (electronic grade)			
PCBM n-type	<b>659169</b>	-3.7 eV	-6.1 eV	



Prod. No.	Fullerene Type	Structure
<b>668184</b>	N-methylfulleropyrrolidine (MP-C <sub>60</sub> )	
<b>658847</b>	(1,2-methanofullerene C <sub>60</sub> )-61-carboxylic acid	

Prod. No.	Fullerene Type	Structure
<b>64245</b>	tert-Butyl (1,2-methanofullerene C <sub>60</sub> )-61-carboxylate	
<b>64247</b>	Diethyl (1,2-methanofullerene C <sub>60</sub> )-61,61-dicarboxylate	
<b>64248</b>	Diethyl (1,2-methanofullerene C <sub>70</sub> )-71,71-dicarboxylate	

## References:

1. Coakley, K.M., McGehee, M.D., *Chem. Mater.*, **2004**, 16, 4533; 2. Thompson, B.C., Kim, Y., Reynolds J.R., *Macromolecules*, **2005**, 38, 5359; 3. Meijer E.J., De Leeuw, D.M., Setayesh, S., Van Veenendaal, E., Huisman, B.-H., Blom, P.W., Hummelen, J.C., Sherf, U., Klapwijk, T.M., *Nat. Mater.*, **2003**, 2, 678; 4. Li, G., Shrotriya, V., Huang, J., Yao, Y., Moriarty, T., Emery, K., Yang, Y., *Nat. Mater.*, **2005**, 4, 864; 5. Guldi, D.M., Luo C., Swartz, A., Gomez, R., Segura, J.L., Martin, N., *J. Phys. Chem. A*, **2004**, 108, 455; 6. Giacalone, F., Segura, J.L., Martin, N., Ramey, J., Guldi, D.M., *Chem. Eur. J.*, **2005**, 11, 4819.

TO ORDER: Contact your local Sigma-Aldrich office (see back cover), call 1-800-325-3010 (USA), or visit [sigma-aldrich.com/matsci](http://sigma-aldrich.com/matsci).

## Carbon Nanotubes Available from Sigma-Aldrich

### Un-functionalized Carbon Nanotubes

Size	Purity (%)	Production Method	Prod. No.
<b>Carbon nanotube, single-walled (SWCNT)</b>			
diam. x length 0.7-1.2 nm x 2-20 µm	10 (as produced)	Produced by CVD Method	<b>589705-1G</b> <b>589705-5G</b>
diam. x length 1.2-1.5 nm x 2-5 µm (bundles)	50	Caborex™ AP-grade	<b>519308-250MG</b> <b>519308-1G</b>
diam. x length 1.2-1.5 nm x 2-5 µm	> 50 (by EDX)	Produced by CVD Method	<b>636797-250MG</b> <b>636797-1G</b>
short SWCNT, diam. x length 0.8-1.5 nm x 0.5 µm	90 (carbon content)	Produced by CVD Method	<b>652512-1G</b>
<b>Carbon nanotubes, multi-walled (MWNT)</b>			
O.D. x I.D. x length 5 nm x 1.3-2.0 nm x 50 µm	50-80	Produced by CVD method	<b>637351-250MG</b> <b>637351-1G</b>
O.D. x wall x length 10-15 nm x 5-15 nm x 0.1-10 µm	> 90 (carbon content)	Product of Arkema, produced by CVD method	<b>677248-5G</b>
O.D. x I.D. x length 10-30 nm x 5-10 nm x 0.5-50 µm	> 95 (carbon content)	Produced by CVD method	<b>636509-2G</b> <b>636509-10G</b> <b>636509-50G</b>
O.D. x I.D. x length 40-70 nm x 5-40 nm x 0.5-2 µm	> 95 (carbon content)	Produced by CVD method	<b>636843-2G</b> <b>636843-50G</b>
diam. x length 110-170 nm x 5-9 µm	> 90 (carbon content)	Produced by CVD method	<b>659258-2G</b> <b>659258-10G</b>

For a complete list of single- and multiwall nanotubes, as well as other carbon nanomaterials, visit [sigma-aldrich.com/nanocarbon](http://sigma-aldrich.com/nanocarbon).

### Functionalized Single-walled Carbon Nanotubes

Nanotube Type	Size	CNT Purity (%)	Solubility (mg/mL)	Prod. No.
SWCNT functionalized with caboxylic acid (3-6% loading)	diam. x length 4-5 nm x 0.5-1.5 µm	80-90	H <sub>2</sub> O 0.1, DMF 1.0	<b>652490-250MG</b> <b>652490-1G</b>
SWCNT coated with polyamino benzoic acid (65 wt.%)	diam. x length 1.1 nm x 0.5-1 µm	70-85	H <sub>2</sub> O 5.0, DMF 0.1, EtOH 0.05	<b>639230-50MG</b>
SWCNT coated with polyethylene glycol (PEG, 30 wt.%)	diam. x length 4-5 nm x 0.5-0.6 µm	80-90	H <sub>2</sub> O 5.0	<b>652474-10MG</b>
SWCNT coated with octadecylamine (ODA, 30-40 wt.%)	diam. x length 2-8 nm x 0.5-1.0 µm	80-90	THF > 1.0, CS <sub>2</sub> > 1.0 benzene > 1.0, toluene > 1.0 1,2-dichlorobenzene > 1.0	<b>652482-10MG</b>

Physisorbed polymers can also be used to functionalize carbon nanotubes, as discussed in the preceding article by Dr. Kim. Sigma-Aldrich offers a wide selection of hydrophilic polymers suitable for CNT functionalization, including low molecular weight polyacrylic acids, polyethylene oxides (also known as poly(ethylene glycols), and polyethylenimines. The table below gives a short selection of these products. For a complete list of hydrophilic polymers visit [sigma-aldrich.com/bicomp](http://sigma-aldrich.com/bicomp).

Polymer	MW (average)	Prod. No.
Poly(acrylic acid)	1,800	<b>323667</b>
Poly(acrylic acid), sodium salt	2,100	<b>420344</b>
Polyacrylamide, 50 wt. % solution in H <sub>2</sub> O	1,500	<b>434930</b>
Poly(ethylene glycol)	850-950	<b>372994</b>
Poly(ethylene glycol)	4,400-4,800	<b>373001</b>
Poly(ethylene glycol) methyl ether methacrylate	1,100	<b>447951</b>
Poly(ethylene glycol)- <i>block</i> -poly(ε-caprolactone)	5,000 PEG / 5,000 caprolactone	<b>570303</b>
Polyethylenimine, 50 wt. % solution in H <sub>2</sub> O	1,300	<b>482595</b>
Polyethylenimine, 50 wt. % solution in H <sub>2</sub> O	2,000	<b>408700</b>

For questions, product data, or new product suggestions, please contact the Materials Science team at [matsci@sial.com](mailto:matsci@sial.com).

## Polymer-Clay Nanocomposites: Design and Application of Multi-Functional Materials



Dr. Alexander B. Morgan  
University of Dayton Research Institute

### Why Use Polymer Nanocomposites?

One of the desirable end-goals of materials science research is the development of multi-functional materials. These materials are defined as compositions that bring more than one property enhancement to a particular application, thus allowing the material to replace more than one other material in an engineered object, or to replace entire classes of materials which alone, are only capable of addressing one end-use need. One example is aerospace wings and fuselages, which today are made of metal. A multi-functional material used to replace the metal would need to be lightweight, very durable to high stress/shear energies, fireproof, and able to conduct electricity to address lightning strike issues at high altitudes. Traditional polymer composites can meet the lightweight and durability requirements and are in use today on aircraft, but they must be combined with metallic meshes and interleaves to address lightning strikes, and they tend to have far worse flammability properties than the metal they replace. The use of nanoparticles in these polymer matrices, thus creating a nanocomposite, can yield an optimal multi-functional material for aerospace needs and other applications.

### Polymer-Clay Nanocomposites

The polymer nanocomposite field has been studied heavily in the past decade, spawning numerous conferences, books, and journal articles. To some extent, it became a major field of study due to key papers from Gianellis and Vaia in the mid-90s<sup>1</sup> and to the release of a commercial polyamide-6 clay nanocomposite by Ube/Toyota of Japan.<sup>2</sup> It can be argued however, that polymer nanocomposite technology has been around for quite some time in the form of latex paints, carbon-black filled tires, and other polymer systems filled with nanoscale particles. However, the nanoscale interface nature of these materials was not truly understood and elucidated until recently. Today, there are excellent review papers and books that cover the entire field of polymer nanocomposite research, including applications, with a wide range of nanofillers such as layered silicates (clays), carbon nanotubes/nanofibers, colloidal oxides, double-layered hydroxides, quantum dots, nanocrystalline metals, and so on.<sup>3</sup> The majority of the research conducted to date has been with organically-treated, layered silicates, or organoclays, and this short review article will focus on polymer nanocomposites made with these materials.

Before describing organoclay structure and chemistry, a rudimentary understanding of the polymer nanocomposite itself is required. A traditional composite containing micron or larger particles/fibers/reinforcement can best be thought of as containing two major components, the bulk polymer and the filler/reinforcement, and a third, very minor component, or interfacial polymer. Poor interfacial bonding between the bulk polymer and filler can result in an undesirable balance of properties, or at worst, material failure under mechanical, thermal, or electrical load. In a polymer nanocomposite, since the reinforcing particle is at the nanometer scale, it is actually a minor component in terms of total weight or volume percent in the final material. If the nanoparticle is fully dispersed in the polymer matrix, the bulk polymer also becomes a minor, and in some cases, a non-existent part of the final material. With the nanofiller homogeneously dispersed in the polymer matrix, the entire polymer becomes an interfacial polymer, and the properties of the material begin to change. Changes in properties of the interfacial polymer become magnified in the final material, and great improvements in properties are seen. Therefore, a polymer nanocomposite is a composite where filler and bulk polymer are minor components, and the interfacial polymer is the component that dictates material properties. With this in mind, the design of the nanoparticle is critical to nanocomposite structure, and careful understanding of nanoparticle chemistry and structure are needed.

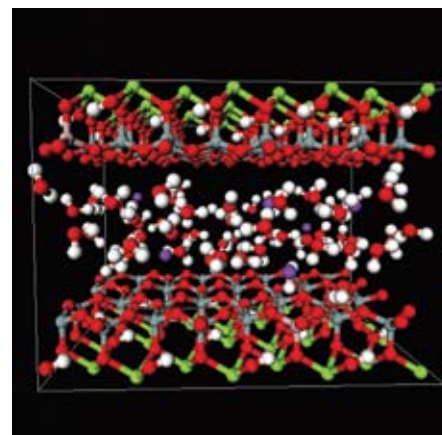
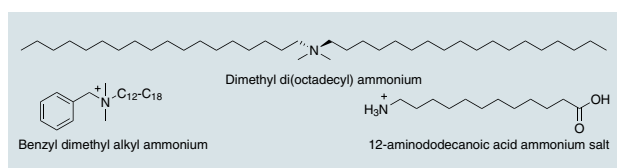


**Figure 1.** Molecular model<sup>5</sup> of Hydrated Montmorillonite clay  $[(Mg_{0.33}Al_{1.67})Si_4O_{10}(OH)_2]Na_{0.33}$ . The clay layers are separated by a layer of water molecules.

## Organoclay Chemistry and Structure

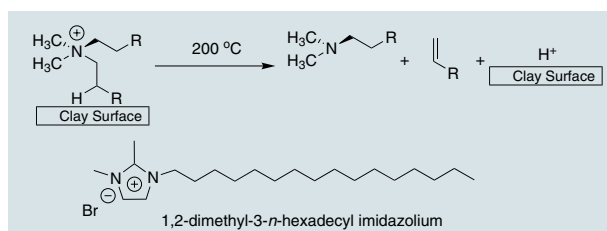
Clays are a broad class of inorganic layered structures. They can occur naturally or be made via synthetic techniques. While many different clay structures have been used in the synthesis of organoclays and polymer-organoclay nanocomposites, the majority of the research has been accomplished with montmorillonite. Montmorillonite is a 2:1 aluminosilicate, meaning it is composed of an octahedral aluminum oxide layer sandwiched between two tetrahedral silicon oxide layers. In the octahedral layer, aluminum atoms are replaced with other cations (e.g., magnesium, iron), which creates some charge defects in the structure (**Figure 1**). This means that montmorillonite has cations associated with its structure to balance this charge in the octahedral layer, and these cations sit atop the silicate tetrahedral layer. Since there is no formal ionic bond between the anionic charge defect in the octahedral layer and the cation on top of the silicate layer (more of a charge association), the cations can be exchanged with other cations of similar charge to generate organically treated clays. Sodium cations on montmorillonite can ion exchange with alkyl ammonium, phosphonium, imidazolium, or any other +1 cation to yield an organoclay (**Scheme 1**). It should be noted that ion exchange with sodium montmorillonite is facile with many different cations, but cations with charges greater than +1 have a strong tendency to lock the clay plates together (a process called pillaring),<sup>4</sup> which renders polymer nanocomposite synthesis impossible.



**Scheme 1.** Typical alkyl ammonium organic treatments

The organic treatment of the clay renders the normally hydrophilic montmorillonite hydrophobic, thus allowing it to interface with many different polymer matrices. Without this organic treatment, the montmorillonite would never disperse into the polymer and remain as micron-sized particles, serving as a traditional filler. The exception to this is when montmorillonite is dispersed in water and mixed with a water soluble polymer such as poly(vinyl alcohol). A good nanocomposite can then be obtained without organic treatment.<sup>6</sup> For almost all other non-water soluble polymers, however, an organic treatment on the clay surface will be needed to obtain a polymer nanocomposite structure. The most commonly used organic treatment is an alkyl ammonium, which can have variety of chain lengths or functionality present, and can be a quaternized primary, secondary, or tertiary amine. The one common feature to a successful clay organic treatment is the presence of at least one long (12 carbons or more) alkyl chain, as without this microcomposites are typically obtained.<sup>7</sup> Care must be taken when picking the organic treatment to allow polymer nanocomposite formation. Due to the variety of structures available, including those which enable polymerization or grafting involving the organic treatment, it is best to refer to the open literature before selecting an organic treatment with which to work. Guides do exist however,<sup>3,8</sup> and these can aid the selection. One final note on organic treatment selection must be made, and that is to consider the thermal stability needed in the final

material application. Alkyl ammoniums, while very successful in the synthesis and development of polymer nanocomposite materials, are thermally unstable above 200 °C, undergoing a Hofmann degradation at this temperature (**Scheme 2**).<sup>9</sup> When this occurs, the polymer/clay interface is destroyed and the material can thermally rearrange to give a microcomposite structure, thus nullifying any gains achieved by the original nanocomposite structure.<sup>10</sup> For higher temperature end use applications, imidazoliums (Scheme 2) appear to have great promise, capable of handling temperatures  $\geq 300$  °C and available in a variety of structures that can be tailored to the polymer nanocomposite application.<sup>11</sup>



**Scheme 2.** Hofmann Degradation of alkyl ammonium on clay surface and thermally stable imidazolium cation treatment.

## Selecting the Organoclay and Analyzing the Nanocomposite

Polymer clay nanocomposites show great promise for materials science applications, but the synthesis and successful development of these materials is not simple. Organoclays are not a “drop-in” solution; careful selection and consideration of the entire nanocomposite system must be undertaken before a successful polymer-clay nanocomposite (or any nanocomposite for that matter) can be prepared and utilized for a new materials science application. If the wrong organoclay is chosen for a particular polymer, the nanocomposite may never be formed, as the nanoparticles might not disperse well enough. Further, even if the best organoclay is chosen, poor mixing or synthetic processes can result in a failure to form a nanocomposite, and in some cases, may result in a material with properties worse than the starting polymer. Finally, the target application will dictate clay loading, or whether a clay is even acceptable for that final application. Therefore, designing the nanocomposite system on paper before actually going to the lab is recommended. Pick an organoclay that will be miscible with the polymer chosen,<sup>12</sup> and will survive the processing conditions. Finally, make sure that the clay property enhancements (mechanical, flammability, gas barrier, etc.) meet with the desired application for the final polymeric material.

Once the system is designed, the material can be prepared, but polymer nanocomposite analysis continues to be just as much a challenge as designing a successful nanocomposite in the first place. No one analytical technique gives all the necessary information about a polymer clay nanocomposite, and some techniques by themselves can give deceptive information on the nature of the clay nanocomposite structure and uniformity of dispersion. In particular, powder x-ray diffraction alone cannot provide the type of information that is required to characterize nanocomposite formation. Several key articles cover this area of nanocomposite analysis,<sup>13</sup> and the researcher is strongly encouraged to read them before embarking on a nanocomposite synthesis program.

Once proper characterization has been obtained, then the researcher can determine if changes need to be made to the process of nanocomposite formulation, or if some other part of the system (such as the clay/polymer interface) is not well-designed and new work is needed.

### Polymer-Clay Nanocomposite Applications

Without going into detail on how the clay nanocomposites impart enhanced property performance, this article will focus on where clay nanocomposites have been used to improve property performance, especially to yield improvement in more than one area, and also where the improvements have led to commercial use. There will be some general discussion about how the properties are obtained, but details are best found in the cited articles or in the review papers cited earlier in this paper.<sup>3</sup>

The most common use of polymer-clay nanocomposites has been in mechanical reinforcement of thermoplastics, especially polyamide-6 and polypropylene. The aforementioned polyamide-6 clay nanocomposite produced by Ube/Toyota was used to replace a metal component near the engine block that yielded some weight savings. The clay in this application improved the heat distortion temperature of the material, allowing it to be used in this higher temperature application. GM/Blackhawk has also announced polypropylene-clay nanocomposites for automotive applications, and the clay brought an increase in flexural/tensile modulus while maintaining impact performance.

The use of polymer-clay nanocomposites for flame retardant applications is becoming more common, especially as it is realized that the clay nanocomposite can replace part of the flame retardant package while maintaining fire safety ratings at a lower flame retardant loading.<sup>14</sup> This results in a better balance of properties for the nanocomposite material compared to the non-nanocomposite flame retardant product, and in some cases, better cost for the flame retardant resin, especially if the organoclay is cheaper than the flame retardant it is replacing. It should be noted that the organoclay can replace traditional flame retardant on more than a 1:1 by weight basis, meaning 1 g of organoclay can replace more than 1 g of traditional flame retardant, resulting in a lighter material. In fact, it appears that clay nanocomposite systems serve as a nearly universal synergist for flame retardant additives, with some exceptions.<sup>14</sup> The synergistic enhancements of clay nanocomposites for fire safety applications has led to two commercial products: a Wire & Cable jacket material (organoclay + aluminum hydroxide) produced by Kabelwerk Eupen AG, and a series of polypropylene + organoclay + flame retardant systems (Maxxam™ FR) produced by PolyOne®. It is likely that other commercial materials will be released soon as more manufacturers begin to see the value of these nanocomposite systems.

Another common application of clay nanocomposites is for gas-barrier materials. Clay nanoparticles create a complex network in the polymer matrix, such that various gases either diffuse very slowly or not at all through polymer chains and pinholes in thin films or thicker polymer parts. The success of clay nanocomposites to impart decreased diffusivity of oxygen and water has led to their use in food/liquid packaging to keep foods fresher longer.<sup>3</sup>

### Future Applications

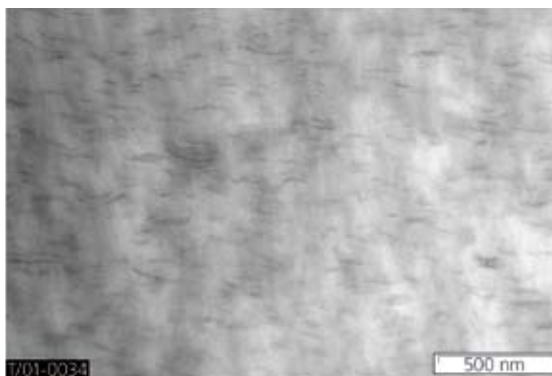
Polymer clay nanocomposites are already used in many applications to enhance existing properties of a particular material, and further R&D efforts should focus on development of true multi-functional materials. Certainly, clay nanocomposites will continue to be used for enhanced mechanical, flammability, and gas barrier properties, but fundamental limits in clay chemistry prevent them from being used easily in applications requiring electrical/thermal conductivity or optical applications. Along those lines, combinations of organoclays with other nanofillers to obtain a true multi-functional material will likely arise in the future. Combining an organoclay with carbon nanotubes, or quantum dots, could yield a very interesting nanocomposite with enhanced mechanical, flammability, thermal, and electrical properties – allowing it to be a drop-in replacement for many different materials in a complex part. Or, the clay could enhance the properties of some existing mechanically fragile system while keeping other properties intact. Some early initial research has been done on combining more than one type of nanofiller in a polymer matrix, but this approach has not yet been widely studied.

The field of polymer-clay nanocomposites, and the broader field of polymer nanocomposites, continues to grow. As stated in the introduction, these materials have likely been in use for quite some time already, but as the chemist and materials scientist become better at designing the system through fundamentals, new products and applications utilizing this technology will grow in number and capability.

### References

- (1) (a) Giannelis, E.P., *Advanced Materials*, **1996**, 8, 29. (b) Vaia, R.A., Jandt, K.D., Kramer, E., Giannelis, E.P., *Chem. Mater.*, **1996**, 8, 2628. (c) LeBaron, P.C., Wang, Z., Pinnavaia, T.J., *Applied Clay Science*, **1999**, 15, 11. (2) (a) Okada, A., Fukushima, Y., Kawasumi, M., Inagaki, S., Usuki, A., Sugiyama, S., Kurauchi, T., Kamigaito, O., U.S. Patent 4,739,007 (1988). (b) Usuki, A., Kojima, Y., Kawasumi, M., Okada, A., Fukushima, Y., Kurauchi, T., Kamigaito, O., *J. Mater. Res.*, **1993**, 8, 1179. (c) Okada, A., Usuki, A., *Mat. Sci. Eng. C.*, **1995**, 3, 109. (3) (a) Utracki, L.A., *Clay-containing Polymeric Nanocomposites*, **2004**, RAPRA Tech. Ltd., Shawbury, Shrewsbury, Shropshire, UK. (b) Ray, S.S., Okamoto, M., *Prog. Polym. Sci.*, **2003**, 28, 1539. (c) Alexandre, M., Dubois, P., *Materials Science and Engineering Reports*, **2000**, 28, 1. (d) Pinnavaia, T.J., Beall, G.W., Eds., *Polymer-Clay Nanocomposites*, **2000**, John Wiley and Sons, Chichester, UK. (4) Lahav, N., Shani, U., Shabtai, J., *Clays and Clay Minerals*, **1978**, 26, 107. (5) <http://www.ill.fr/dif/3D-crystals/layers.html> (6) Strawhecker, K.E., Manias, E., *Chem. Mater.*, **2000**, 12, 2943. (7) (a) Zilg, C., Thomann, R., Finter, J., Mulhaupt, R., *Macromol. Mater. Eng.*, **2000**, 280/281, 41. (b) Reichert, P., Nitz, H., Klinke, S., Brandsch, R., Thomann, R., Mulhaupt, R., *Macromol. Mater. Eng.*, **2000**, 275, 8. (8) [http://www.nanocor.com/tech\\_sheets.asp](http://www.nanocor.com/tech_sheets.asp) (9) Xie, W., Gao, Z., Pan, W.P., Hunter, D., Singh, A., Vaia, R., *Chem. Mater.*, **2001**, 13, 2979. (10) (a) Shah, R.K., Paul, D.R., *Polymer*, **2006**, 47, 4084. (b) Nassar, N., Utracki, L.A., Kamal, M., *Intl. Polym. Proc.*, **2005**, XX, 423. (c) Gilman, J.W., Jackson, C.L., Morgan, A.B., Harris, R., Manias, E., Giannelis, E.P., Wuthenow, M., Hilton, D., Phillips, S.H., *Chem. Mater.*, **2000**, 12, 1866. (11) (a) Gilman, J.W., Awad, W.H., Davis, R.D., Shields, J., Harris, Jr., R.H., Davis, C., Morgan,

A.B., Sutto, T.E., Callahan, J., Trulove, P.C., DeLong, H.C., *Chem. Mater.*, **2002**, *14*, 3776. (b) Bottino, F.A., Fabbri, E., Fragala, I.L., Malandrino, G., Orestano, A., Pilati, F., Pollicino, A., *Macromol. Rapid Commun.*, **2003**, *24*, 1079. (c) Wang, Z.M., Chung, T.C., Gilman, J.W., Manias, E., *J. Polym. Sci. Part B.*, **2003**, *41*, 3173. (d) Davis, R.D., Gilman, J.W., Sutto, T.E., Callahan, J.H., Trulove, P.C., De Long, H.C., *Clays and Clay Minerals*, **2004**, *52*, 171. (12) Jang, B.N., Wang, D., Wilkie, C.A., *Macromolecules*, **2005**, *38*, 6533. (13) (a) Morgan, A.B., Gilman, J.W., *J. App. Polym. Sci.*, **2003**, *87*, 1329. (b) Perrin-Sarazin, F., Ton-That, M.T., Bureau, M.N., Denault, J., *Polymer*, **2005**, *46*, 11624. (c) Vermogen, A., Masenelli-Varlot, K., Seguela, R., Duchet-Rumeau, J., Boucard, S., Prele, P., *Macromolecules*, **2005**, *38*, 9661. (14) Morgan, A.B., *Polym. Adv. Technol.*, **2006**, *17*, 206.



Transmission Electron Micrograph of a nylon nanocomposite with 2% Nanoclay Nanomer®, I34TCN (**682640**).

## Sigma-Aldrich Nanoclays

Sigma-Aldrich, in partnership with Nanocor Corporation, is pleased to offer a versatile set of montmorillonite Nanomer® nanoclays. These materials are optimized for incorporation into a broad range of polymer blends, with suggested usage methodology available in up-to-date Technical Datasheets.

Product Name*	Product Description	Technical Datasheet Code	Method of Incorporation	Application (Polymer Systems)	Property Improved	Prod. No.
Nanoclay, Nanomer® I.28E	montmorillonite clay modified with 25-30 wt.% trimethyl stearyl ammonium	T12, T14, T17	See Tech Datasheet	Epoxy (anhydride-cured)	<ul style="list-style-type: none"> <li>- Speed up cure catalyst</li> <li>- Improve modulus</li> <li>- Increase Tg</li> <li>- Enhance Chemical resistance</li> <li>- Rheology control</li> </ul>	<b>682608</b>
Nanoclay, Nanomer® I.30E	montmorillonite clay surface modified with 25-30 wt.% octadecylamine	T11, T13	See Tech Datasheet	Epoxy (Amine-cured), Polyurethane	<ul style="list-style-type: none"> <li>- Speed up cure catalyst</li> <li>- Improve modulus</li> <li>- Increase Tg</li> <li>- Enhance Chemical resistance</li> </ul>	<b>682616</b>
Nanoclay, Nanomer® I.44P	montmorillonite clay surface modified with 35-45 wt.% dimethyl dialkyl(C14-C18) amine	P801, P804	Recommended for melt compounding	PP: Polypropylene PE: Polyethylene EVA: Ethylene Vinyl Acetate	<ul style="list-style-type: none"> <li>- Improve modulus</li> <li>- Increase barrier</li> <li>- Enhance chemical resistance</li> <li>- Improve flame retardancy</li> <li>- Increase HDT (heat deflection temperature)</li> </ul>	<b>682624</b>
Nanoclay, Nanomer® I.31PS	montmorillonite clay surface modified with 15-35 wt.% octadecylamine and 0.5-5 wt.% aminopropyltriethoxysilane	P801, P804 (Improved thermal stability vs. I.44P)	Recommended for melt compounding	PP: Polypropylene PE: Polyethylene EVA: Ethylene Vinyl Acetate	<ul style="list-style-type: none"> <li>- Improve modulus</li> <li>- Increase barrier</li> <li>- Enhance chemical resistance</li> <li>- Improve flame retardancy</li> <li>- Increase HDT (heat deflection temperature)</li> </ul>	<b>682632</b>
Nanoclay, Nanomer® I.34TCN	montmorillonite clay surface modified with 25-30wt% methyl dihydroxyethyl hydrogenated tallow ammonium	N605	Recommended for melt compounding	Nylon 6, 66 and other polyamide	<ul style="list-style-type: none"> <li>- Improve modulus</li> <li>- Increase barrier</li> <li>- Enhance chemical resistance</li> <li>- Increase HDT (heat deflection temperature)</li> </ul>	<b>682640</b>
Nanoclay, Nanomer® PGV	hydrophilic bentonite nanoclay (no organic modification)	G105	Dispersion in water	Untreated hydrophilic clay for dispersion in water-based polymers and coatings.	<ul style="list-style-type: none"> <li>- Rheology control</li> <li>- Increase barrier</li> <li>- Enhance Chemical Resistance</li> </ul>	<b>682659</b>

\*Nanomer® clays are products of Nanocor Corporation.

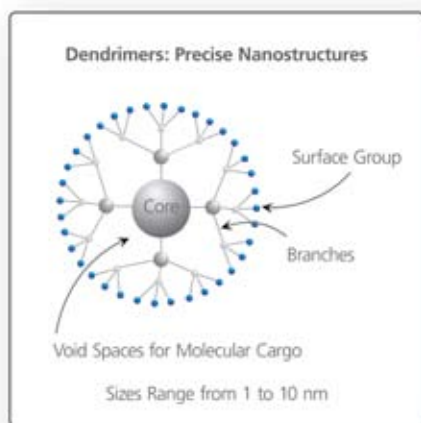
For questions, product data, or new product suggestions, please contact the Materials Science team at [matsci@sial.com](mailto:matsci@sial.com).

## Solubility Enhancement of Poorly Water Soluble Molecules using Dendrimers



Dr. Abhay Singh Chauhan, Dr. Sonke Svenson, Dr. Lori Reyna, and Dr. Donald Tomalia, CTO; Dendritic Nanotechnologies, Inc.

Environmental concerns are driving the replacement of volatile organic solvents by water and aqueous mixtures. This change often creates challenges because many organic molecules show low water solubility. In addition, in some applications it is necessary to mix hydrophilic and hydrophobic components in one formulation, requiring the use of solubility modifiers. Dendrimers can provide a solution in both scenarios. Dendrimers are core-shell nanostructures with precise architecture and low polydispersity, which are synthesized in a generation-by-generation fashion around a core unit, resulting in a high level of control over size, branching points, and surface functionality (**Drawing 1**).<sup>1</sup> The ability to tailor dendrimer properties to the needs of a guest molecule makes them ideal carriers for molecular encapsulation, allowing dissolution of hydrophobic materials in water and mixing of hydrophilic and hydrophobic compounds, for example in catalytic applications.<sup>2</sup>



**Drawing 1.** Schematic representation of a G2 dendrimer with 3-fold branching. PAMAM dendrimers have 2-fold branching, resulting in 2x increase in number of surface groups with each generation, G.

In this article, we demonstrate the ability of dendrimers to improve water solubility using two poorly water-soluble drugs as model materials. Low water solubility, and therefore, poor bioavailability, are a major challenge in drug delivery.<sup>3</sup> The anti-cancer drug cisplatin and the non-steroidal anti-inflammatory drug indomethacin have been encapsulated into STARBURST® poly(amidoamine) (PAMAM) dendrimers, and their encapsulation efficiency and release profiles have been studied. Compared to control experiments without dendrimers, dendrimer-drug formulations showed up to 37-fold drug solubility enhancement.

### Experimental

**Materials.** STARBURST® PAMAM dendrimers are products of Dendritic Nanotechnologies, Inc and available through Sigma-Aldrich. All other reagents and solvents are available from Sigma-Aldrich and were used as received.

**Encapsulation Protocol.** Dendrimers were dissolved in deionized (DI) water and mixed with excess drug. These suspensions were briefly exposed to ultrasonication, and then incubated overnight at 37° C and 100 rpm in a shaking water bath. After equilibration to ambient temperature, the dendrimer-drug suspensions were filtered through a 0.2- $\mu$ m nylon syringe filter to remove excess solid drug. Non-encapsulated drug was removed by dialysis using a 1-kDa cutoff membrane against DI water at 4° C for 30 min. Drug samples were freeze-dried and analyzed for encapsulated drug content by UV spectroscopy at 320 nm using a Perkin Elmer™ Lambda 2 UV/VIS Spectrophotometer (indomethacin) or by inductively coupled plasma (ICP) spectroscopy (cisplatin). Procedure was performed in triplicate.

**In Vitro Release Protocol.** Dendrimer-drug conjugates were re-dissolved in DI water or saline solution and placed in a dialysis bag using a 1-kDa cutoff membrane at 37° C. At certain time intervals, aliquots were removed from the outer dialysis compartment, freeze-dried and analyzed by UV spectroscopy or ICP as described above.

## Results and Discussion

### Cisplatin

Encapsulation of cisplatin is independent of dendrimer core and generation as evident from **Table 1** ( $P > 0.05$ ). The effect of drug/dendrimer molar ratios on the percentage of Pt content was studied using dendrimer G3.5 with diaminoethane (EDA) core and sodium carboxylate surface groups. Increasing the cisplatin/dendrimer molar ratio resulted in enhanced Pt content of the dendrimer formulations (**Table 2**). The effect of dendrimer-to-cisplatin loading on *in vitro* release was studied using dendrimer G3.5 (**Figure 1**). The release rate was correlated to the amount of drug loaded into the dendrimers, with fast release at high loading but slow release (long retention time) at low loading. Long retention is desirable in technical, catalytic applications. *In vitro* release of cisplatin was independent of the dendrimer core size. The release profiles in saline solution (high ionic strength) were similar to the release profiles in DI water (data not shown).

**Table 1:** Effect of core and generation on cisplatin loading of dendrimers.

Core	Dendrimer Gen	Pt content (%w/v) Mean $\pm$ SD	Prod. No.
EDA <sup>a</sup>	3.5	27.27 $\pm$ 0.67	412430
EDA	4.5	27.6 $\pm$ 1.21	470457
DAB <sup>b</sup>	4.5	27.7 $\pm$ 0.53	635618
DOD <sup>c</sup>	3.5	26.7 $\pm$ 1.4	635480
DOD	4.5	25.02 $\pm$ 0.39	635472

<sup>a</sup>diaminoethane; <sup>b</sup>diaminobutane; <sup>c</sup>diaminododecane

**Table 2:** The effect of drug/dendrimer molar ratio on the percentage of Pt content (STARBURST<sup>®</sup> dendrimer G3.5 with EDA core and COONa surface).

Drug/dendrimer molar ratio	Pt content (%w/v)
9.4	10.92
19	18.65
28	26.19
53	35.8
78	42.8
106	50.1
304	58.05

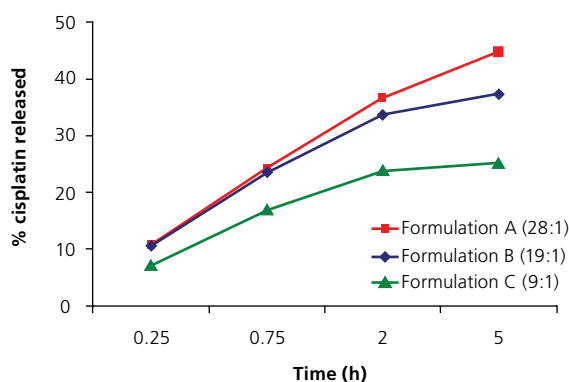


**Figure 1.** *In vitro* release profiles of cisplatin formulated with STARBURST<sup>®</sup> dendrimer G3.5 sodium carboxylate surface in DI water at different molar ratios. Ratio listed next to formulation denotes number of drug molecules associated with dendrimer.

### Indomethacin

STARBURST<sup>®</sup> dendrimers of different generations (G1-6) and surface groups have been used to study encapsulation and release of indomethacin (**Figure 2**). Water solubility of indomethacin was dramatically enhanced through encapsulation, depending on dendrimer size ( $G6 > G5 > G4 > G3$ ) and surface groups ( $NH_2 > OH > COO^-$ ). *In vitro* release of indomethacin showed a similar but inverted relationship to size ( $G3 > G4 > G5 > G6$ ) and surface groups ( $NH_2 < OH < COO^-$ ) (**Figure 3**). Lag time and very slow release from STARBURST<sup>®</sup> dendrimer G4 with amine surface groups is a result of strong electrostatic interactions and hydrogen bonding of indomethacin between dendrimer surface and the carboxylate group of the drug. Fast release from STARBURST<sup>®</sup> dendrimer G4 with sodium carboxylate surface groups reflects electrostatic repulsion between adjacent surface groups. This repulsion opens the dendritic structure and reduces its container properties, as well as repulsion between drug molecules and dendrimer surface. However, drug release can be slowed down by modification of the dendrimer surface, e.g., by surface conjugation of poly(ethylene glycol) chains such as PEG-500. Such PEG-modified dendrimers are now commercially available (See PEG dendrimer kit **683493**).

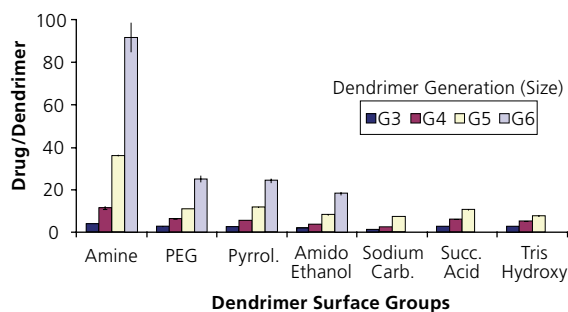


**Figure 2.** Encapsulation efficiency of indomethacin into STARBURST<sup>®</sup> dendrimers. Different dendrimer surfaces shown: primary amine, poly(ethylene glycol), carbomethoxypyrrolidinone, amidoethanol, sodium carboxylate, succinamic acid, and tris(hydroxymethyl)amidomethane.

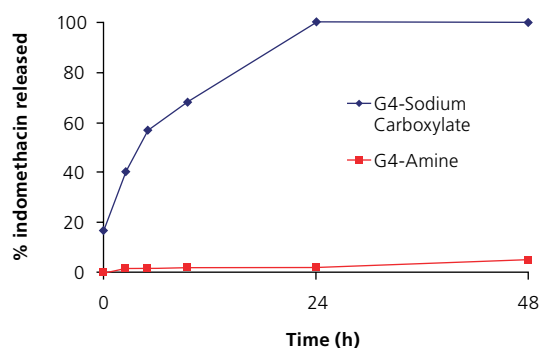


**Figure 3.** Indomethacin release from STARBURST<sup>®</sup> dendrimers G4 with primary amine and sodium carboxylate surface groups.

### Comparison of Release Profiles

Release of the drug from the dendrimer matrix depends upon the nature of the drug and its interactions with the dendrimer. For example, the repulsive interaction between the dendritic carrier and indomethacin mentioned above results in fast release of this drug from PAMAM® dendrimers G4 with carboxylate surface groups compared to cisplatin (56.9% versus 25.3% after 5 h). Consequently, release profiles can be tailored to the application needs by choice of the dendrimer surface groups (e.g., amine versus carboxylate) as well as the drug/dendrimer molar ratio (Figures 1 and 3). Judicious selection of the dendrimer therefore can control the release profile of the encapsulated material.

**Table 3:** Aldrich Product numbers for products used in indomethacin solubility study.

Dendrimer	Amine (Amino)	Hydroxy (amidoethanol)	Sodium Carboxylate
G3	596094	635197	635634
G4	596191	635200	635626
G5	596302	635219	635618
G6	596426	635227	635596

### Conclusion

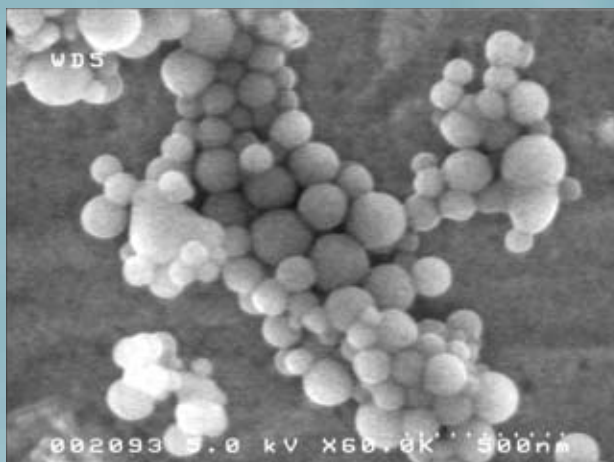
Formulation of poorly water-soluble drugs with STARBURST® PAMAM dendrimers resulted in increased water solubility, and therefore, enhanced bioavailability of these drugs. This behavior has been demonstrated for two drug classes, small metal ion containing drugs such as cisplatin, and organic molecules such as indomethacin. However, these properties of dendrimers are not restricted to drug molecules but can also be applied to catalysts and organic molecules, where dendrimers function as solubility enhancer and modifier, allowing to mix otherwise immiscible materials.<sup>2</sup> Dendritic Nanotechnologies' new Priostar™ dendrimer family provides these carriers at low cost and enhanced thermal and hydrolytic stability compared to STARBURST® PAMAM dendrimers, making them ideal candidates for commercializing industrial applications.

### References

(1) D.A. Tomalia, *Aldrichimica Acta*, **2004**, 37, 39. (2) S. Svenson, *Kirk-Othmer Encyclopedia of Chemical Technology*, 5th ed., **2007**, 26, 786. (3) S. Svenson, D.A. Tomalia, *Advanced Drug Delivery Reviews*, **2005**, 57, 2106.

## Nanomaterials for Biomedical Applications

Dendrimers are just one class of nano-sized materials that are explored to develop new life-saving technologies. Single-wall carbon nanotubes, described on page 16, are used to make miniaturized sensors for DNA, pathogens, and chemicals – for example glucose sensors. Multi-wall nanotubes, nanoclays, and ceramic nanoparticles are incorporated in ultra-strong polymer nanocomposites that will be used in orthopedic, for example joint-replacement, applications. Nanoparticles can also be used to make nano-textured substrates to support attachment and growth of cells for tissue engineering. Hydroxyapatite nanopowders (**677418**), incorporated in biodegradable polymer composites<sup>1</sup> or deposited on biocompatible substrates,<sup>2</sup> have been shown to promote adhesion and proliferation of bone-forming (osteoblast) cells. Sigma-Aldrich is looking forward to bring you new nanomaterials tools to accelerate research in biotechnology and medicine – please let us know how we can help: [matsci@sial.com](mailto:matsci@sial.com).



#### 677418 Hydroxyapatite Nanopowder

- Molecular Formula  $[Ca_5(OH)(PO_4)_3]_x$
- Average Particle Size 150 – 200 nm
- Surface Area > 9.4 m<sup>2</sup>/g
- Available in 5g pack size

#### References:

(1) Kim, S.; Park, M.; Jeon, O.; Choi, C.; Kim, B., *Biomaterials* **2006**, 27, 1399. (2) Sato, M.; Sambito M.; Aslani, A.; Kalkhoran, N.; Slamovich, E.; Webster, T., *Biomaterials* **2006**, 27, 2358.

## Dendrimer Kits Available from Sigma-Aldrich

Sigma-Aldrich is pleased to offer dendrimer kits. Each kit offers a set of structurally related dendrimers in convenient small quantities designed to facilitate your research. Larger quantities of individual dendrimers can be purchased from the Sigma-Aldrich catalog, once you have identified compounds successful in your application. Note that the diameter as well as number of surface functional groups (valency) of the dendrimers increase with the generation G. For a complete list of available dendrimers, visit [sigma-aldrich.com/dendrimer](http://sigma-aldrich.com/dendrimer).

### 664138 PAMAM Dendrimer Kit, Generations 0-3, ethylenediamine (2-carbon) core \*

Name	Kit Quantity	Generation	MW (calc.)	Est. Diam. (Å)	Surface Groups
PAMAM-Gen 0	5 wt.% in 1mL methanol	0	517	15	4 X amine (-NH <sub>2</sub> )
PAMAM-Gen 1	5 wt.% in 1mL methanol	1	1,430	22	8 X amine (-NH <sub>2</sub> )
PAMAM-Gen 2	5 wt.% in 1mL methanol	2	3,256	29	16 X amine (-NH <sub>2</sub> )
PAMAM-Gen 3	5 wt.% in 1mL methanol	3	6,909	36	32 X amine (-NH <sub>2</sub> )

### 664049 PAMAM Dendrimer Kit, Generations 4-7, ethylenediamine (2-carbon) core \*

Name	Kit Quantity	Generation	MW (calc.)	Est. Diam. (Å)	Surface Groups
PAMAM-Gen 4	5 wt.% in 1mL methanol	4	14,215	15	64 X amine (-NH <sub>2</sub> )
PAMAM-Gen 5	5 wt.% in 1mL methanol	5	28,826	22	128 X amine (-NH <sub>2</sub> )
PAMAM-Gen 6	5 wt.% in 1mL methanol	6	58,048	29	256 X amine (-NH <sub>2</sub> )
PAMAM-Gen 7	5 wt.% in 1mL methanol	7	116,493	36	512 X amine (-NH <sub>2</sub> )

### 683493 PEG-Dendrimer Kit, Generations 3-6, 1,4-diaminobutane (4-carbon) core \*\*

Name	Kit Quantity	Generation	MW (calc.)	Est. Diam. (Å)	Surface Groups
PAMAM-G3-PEG	10 wt.% in 0.5 mL methanol	3	25,711	4.0	32 X PEG-12
PAMAM-G4-PEG	10 wt.% in 0.5 mL methanol	4	51,782	5.0	64 X PEG-12
PAMAM-G5-PEG	10 wt.% in 0.5 mL methanol	5	103,933	6.5	128 X PEG-12
PAMAM-G6-PEG	10 wt.% in 0.5 mL methanol	6	208,234	8.0	256 X PEG-12

PEG-12 = (COO(CH<sub>2</sub>CH<sub>2</sub>O)<sub>12</sub>CH<sub>3</sub>)

### 683507 Hydrophilic-Dendrimer Kit, Generation 4, 1,4-diaminobutane (4-carbon) core \*\*

Name	Kit Quantity	Generation	MW (calc.)	Est. Diam. (Å)	Surface Groups
PAMAM-G4-OH	10 wt.% in 0.5 mL methanol	4	14,297	4.6	64 X amidoethanol
PAMAM-G4-NH <sub>2</sub>	10 wt.% in 0.5 mL methanol	4	14,234	4.5	64 X amine
PAMAM-G5-PEG	10 wt.% in 0.5 mL methanol	4	51,782	5.0	64 X PEG-12
PAMAM-G6-COOH	10 wt.% in 0.5 mL methanol	4	20,635	4.8	64 X succinamic acid

\* Manufactured by Dendritech, Inc.

\*\* Manufactured by Dendritic Nanotechnologies, Inc.

Dendrimers for  
Drug Delivery

Order: 1.800.325.3010 Technical Service: 1.800.231.8327

**ALDRICH**

For questions, product data, or new product suggestions,  
please contact the Materials Science team at [matsci@sial.com](mailto:matsci@sial.com).

**Argentina**

SIGMA-ALDRICH DE ARGENTINA S.A.  
Free Tel: 0810 888 7446  
Tel: (+54) 11 4556 1472  
Fax: (+54) 11 4552 1698

**Australia**

SIGMA-ALDRICH PTY LTD.  
Free Tel: 1800 800 097  
Free Fax: 1800 800 096  
Tel: (+61) 2 9841 0555  
Fax: (+61) 2 9841 0500

**Austria**

SIGMA-ALDRICH HANDELS GmbH  
Tel: (+43) 1 605 81 10  
Fax: (+43) 1 605 81 20

**Belgium**

SIGMA-ALDRICH NV/SA.  
Free Tel: 0800 14747  
Free Fax: 0800 14745  
Tel: (+32) 3 899 13 01  
Fax: (+32) 3 899 13 11

**Brazil**

SIGMA-ALDRICH BRASIL LTDA.  
Free Tel: 0800 701 7425  
Tel: (+55) 11 3732 3100  
Fax: (+55) 11 5522 9895

**Canada**

SIGMA-ALDRICH CANADA LTD.  
Free Tel: 1800 565 1400  
Free Fax: 1800 265 3858  
Tel: (+1) 905 829 9500  
Fax: (+1) 905 829 9292

**China**

SIGMA-ALDRICH (SHANGHAI)  
TRADING CO. LTD.  
Free Tel: 800 819 3336  
Tel: (+86) 21 6141 5566  
Fax: (+86) 21 6141 5567

**Czech Republic**

SIGMA-ALDRICH S.R.O.  
Tel: (+420) 246 003 200  
Fax: (+420) 246 003 291

**Denmark**

SIGMA-ALDRICH DENMARK A/S  
Tel: (+45) 43 56 59 10  
Fax: (+45) 43 56 59 05

**Finland**

SIGMA-ALDRICH FINLAND OY  
Tel: (+358) 9 350 9250  
Fax: (+358) 9 350 92555

**France**

SIGMA-ALDRICH CHIMIE S.à.r.l.  
Free Tel: 0800 211 408  
Free Fax: 0800 031 052  
Tel: (+33) 474 82 28 00  
Fax: (+33) 474 95 68 08

**Germany**

SIGMA-ALDRICH CHEMIE GmbH  
Free Tel: 0800 51 55 000  
Free Fax: 0800 64 90 000  
Tel: (+49) 89 6513 0  
Fax: (+49) 89 6513 1160

**Greece**

SIGMA-ALDRICH (O.M.) LTD.  
Tel: (+30) 210 994 8010  
Fax: (+30) 210 994 3831

**Hungary**

SIGMA-ALDRICH Kft  
Ingyenes zöld telefon: 06 80 355 355  
Ingyenes zöld fax: 06 80 344 344  
Tel: (+36) 1 235 9055  
Fax: (+36) 1 235 9050

**India**

SIGMA-ALDRICH CHEMICALS  
PRIVATE LIMITED  
Telephone  
Bangalore: (+91) 80 6621 9600  
New Delhi: (+91) 11 4165 4255  
Mumbai: (+91) 22 2570 2364  
Hyderabad: (+91) 40 6684 5488  
Fax  
Bangalore: (+91) 80 6621 9650  
New Delhi: (+91) 11 4165 4266  
Mumbai: (+91) 22 2579 7589  
Hyderabad: (+91) 40 6684 5466

**Ireland**

SIGMA-ALDRICH IRELAND LTD.  
Free Tel: 1800 200 888  
Free Fax: 1800 600 222  
Tel: (+353) 1 404 1900  
Fax: (+353) 1 404 1910

**Israel**

SIGMA-ALDRICH ISRAEL LTD.  
Free Tel: 1 800 70 2222  
Tel: (+972) 8 948 4100  
Fax: (+972) 8 948 4200

**Italy**

SIGMA-ALDRICH S.r.l.  
Numero Verde: 800 827018  
Tel: (+39) 02 3341 7310  
Fax: (+39) 02 3801 0737

**Japan**

SIGMA-ALDRICH JAPAN K.K.  
Tokyo Tel: (+81) 3 5796 7300  
Tokyo Fax: (+81) 3 5796 7315

**Korea**

SIGMA-ALDRICH KOREA  
Free Tel: (+82) 80 023 7111  
Free Fax: (+82) 80 023 8111  
Tel: (+82) 31 329 9000  
Fax: (+82) 31 329 9090

**Malaysia**

SIGMA-ALDRICH (M) SDN. BHD  
Tel: (+60) 3 5635 3321  
Fax: (+60) 3 5635 4116

**Mexico**

SIGMA-ALDRICH QUÍMICA, S.A. de C.V.  
Free Tel: 01 800 007 5300  
Free Fax: 01 800 712 9920  
Tel: 52 722 276 1600  
Fax: 52 722 276 1601

**The Netherlands**

SIGMA-ALDRICH CHEMIE BV  
Free Tel: 0800 022 9088  
Free Fax: 0800 022 9089  
Tel: (+31) 78 620 5411  
Fax: (+31) 78 620 5421

**New Zealand**

SIGMA-ALDRICH NEW ZEALAND LTD.  
Free Tel: 0800 936 666  
Free Fax: 0800 937 777  
Tel: (+61) 2 9841 0555  
Fax: (+61) 2 9841 0500

**Norway**

SIGMA-ALDRICH NORWAY AS  
Tel: (+47) 23 17 60 60  
Fax: (+47) 23 17 60 50

**Poland**

SIGMA-ALDRICH Sp. z o.o.  
Tel: (+48) 61 829 01 00  
Fax: (+48) 61 829 01 20

**Portugal**

SIGMA-ALDRICH QUÍMICA, S.A.  
Free Tel: 800 202 180  
Free Fax: 800 202 178  
Tel: (+351) 21 924 2555  
Fax: (+351) 21 924 2610

**Russia**

SIGMA-ALDRICH RUS, LLC  
Tel: +7 (495) 621 6037  
Fax: +7 (495) 621 5923

**Singapore**

SIGMA-ALDRICH PTE. LTD.  
Tel: (+65) 6779 1200  
Fax: (+65) 6779 1822

**South Africa**

SIGMA-ALDRICH  
SOUTH AFRICA (PTY) LTD.  
Free Tel: 0800 1100 75  
Free Fax: 0800 1100 79  
Tel: (+27) 11 979 1188  
Fax: (+27) 11 979 1119

**Spain**

SIGMA-ALDRICH QUÍMICA, S.A.  
Free Tel: 900 101 376  
Free Fax: 900 102 028  
Tel: (+34) 91 661 99 77  
Fax: (+34) 91 661 96 42

**Sweden**

SIGMA-ALDRICH SWEDEN AB  
Tel: (+46) 8 742 4200  
Fax: (+46) 8 742 4243

**Switzerland**

SIGMA-ALDRICH CHEMIE GmbH  
Free Tel: 0800 80 00 80  
Free Fax: 0800 80 00 81  
Tel: (+41) 81 755 2828  
Fax: (+41) 81 755 2815

**United Kingdom**

SIGMA-ALDRICH COMPANY LTD.  
Free Tel: 0800 717 181  
Free Fax: 0800 378 785  
Tel: (+44) 1747 833 000  
Fax: (+44) 1747 833 313  
SAFC (UK) Free Tel: 0800 71 71 17

**United States**

SIGMA-ALDRICH  
P.O. Box 14508  
St. Louis, Missouri 63178  
Toll-Free: 800 325 3010  
Toll-Free Fax: 800 325 5052  
Call Collect: (+1) 314 771 5750  
Tel: (+1) 314 771 5765  
Fax: (+1) 314 771 5757

**Internet**

sigma-aldrich.com

**World Headquarters**

3050 Spruce St., St. Louis, MO 63103  
(314) 771-5765  
sigma-aldrich.com

**Order/Customer Service** (800) 325-3010 • Fax (800) 325-5052

**Technical Service** (800) 325-5832 • sigma-aldrich.com/techservice

**Development/Bulk Manufacturing Inquiries SAFC™** (800) 244-1173

**The SIGMA-ALDRICH Group**

©2007 Sigma-Aldrich Co. All rights reserved.

SIGMA, SAFC, SAFC™, SIGMA-ALDRICH, ISOTEC, ALDRICH, FLUKA, and SUPELCO are trademarks belonging to Sigma-Aldrich Co. and its affiliate Sigma-Aldrich Biotechnology, L.P. Riedel-de Haën® trademark under license from Riedel-de Haën GmbH. Sigma brand products are sold through Sigma-Aldrich, Inc. Sigma-Aldrich, Inc. warrants that its products conform to the information contained in this and other Sigma-Aldrich publications. Purchaser must determine the suitability of the product(s) for their particular use. Additional terms and conditions may apply. Please see reverse side of the invoice or packing slip.



Accelerating Customers' Success  
through Leadership in Life Science,  
High Technology and Service

**SIGMA-ALDRICH™**

3050 Spruce Street • St. Louis, MO 63103 USA

J11  
02039-503403  
0027